fused with artificial cerebrospinal fluid at a flow rate of 2.0 μL/min. The artificial cerebrospinal fluid prepared with analytical grade reagents consisted of KCl 2.5 mM, NaCl 125 mM, $MgCl{\cdot}6H_2O$ 1.0 mM, $NaHPO_4{\cdot}2H_2O$ 0.5 mM, $NaH_2PO_4{\cdot}12H_2O$ 2.5 mM, and $CaCl_2$ 1.2 mM.

Sampling was started 60 min after implantation of the probe for stabilization. Samples were then collected twice at 10-min intervals as baselines. Drugs were then administered to rats and samples were taken every 10 min until 3 h and then collected every 1 h for the next 7 h into a sampling tube containing 5 or 30 μL of 0.1 M phosphate buffer (pH 3.5) containing 0.1 M EDTA·2Na (dialysate/phosphate buffer = 4:1 (v/v)).

The *in vivo* recoveries of the probe ($R_{in\ vivo}$) were calculated from three replicate measurements of *in vitro* recoveries ($R_{in\ vitro}$), *in vitro* losses ($L_{in\ vitro}$), and *in vivo* losses ($L_{in\ vivo}$), according to previous reports (Sun et al., 2002; Wada et al., 2008). For these calculations, we used artificial cerebrospinal fluid with the following substances added to be: MDMA (100 ng/mL), MDA (50 ng/mL), methamphetamine (100 ng/mL), amphetamine (50 ng/mL), dopamine (25 nM), and serotonin (25 nM). The relative $R_{in\ vitro}$, $L_{in\ vitro}$, and $L_{in\ vivo}$ values were calculated to be 19.0 ± 4.9%, 41.7 ± 7.5%, and 26.6 ± 4.1% for MDMA; 16.6 ± 5.6%, 45.5 ± 11.3%, and 26.2 ± 3.8% for MDA; 17.8 ± 6.2%, 41.9 ± 7.6%, and 25.8 ± 3.6% for methamphetamine; 17.3 ± 3.2%, 46.0 ± 12.1%, and 29.0 ± 4.0% for amphetamine; 8.5 ± 4.8%, 96.6 ± 1.4%, and 96.9 ± 0.4% for dopamine; and 14.4 ± 2.5%, 95.0 ± 1.6%, and 99.1 ± 0.1% for serotonin, respectively. The percent *in vivo* recoveries for MDMA, MDA, methamphetamine, amphetamine, dopamine, and serotonin were estimated at 12.4%, 10.1%, 11.5%, 11.3%, 8.5%, and 15.0%, respectively.

2.5. Drug administration

MDMA (12 and 25 mg/kg) or methamphetamine (10 mg/kg) in 0.9% saline was i.p. administered to rats at 0.1 mL/100 g body weight. For co-administration of the two drugs, methamphetamine was given immediately following administration of MDMA. For sole administration of MDMA or methamphetamine, saline was injected immediately following administration of either drug to remove the influence of second injection. According to interspecies dose scales (McCann and Ricaurte, 2001), the dose of MDMA used in this study (12 mg/kg) is equivalent to a dose of 164 mg in a 70-kg human. Because the MDMA content of seized tablets ranges from 1 to 245 mg/tablet (Makino et al., 2003; Teng et al., 2006; Morefield et al., 2011), the dose of 12 mg/kg of MDMA is in the range of being abused by humans. In the present study, an MDMA dose of 25 mg/kg was used to determine whether MDMA risks increased in a dose-dependent manner.

2.6. Determination of drugs by HPLC-fluorescence detection

Fluorescence derivatization was performed on 10 μL of samples using DIB-Cl (Tomita et al., 2007) with some modifications. As the internal standard, we added 5 μL of MPPA in methanol to a vial and evaporated the methanol with nitrogen gas. Next, 10 μL of sample, 5 μL of 0.1 M carbonate buffer (pH 10.0) and 90 μL of 0.1 mM DIB-Cl in acetonitrile were added and let stand for 10 min at room temperature. We then added 5 μL of 25% ammonia solution to stop the reaction.

The HPLC-fluorescence system consisted of two chromatographic pumps (LC-$10AT_{VP}$ and LC-10AS, Shimadzu, Kyoto, Japan). One was used for analysis and the other for washing the column, a Rheodyne 7725 injector with a 20 μL sample loop (Rheodyne, CA, USA), a Wakopak Handy octadecylsilica (ODS) column (150 × 4.6 mm, i.d., Wako Pure Chemical Inc.), and an RF-$10A_{XL}$ fluorescence detector set at 330 nm (λ_{ex}) and 440 nm (λ_{em}) (Shimadzu).

The drugs were separated with a mixture of 50 mM phosphate buffer (pH 7.0)/acetonitrile/methanol/2-propanol (=50:45:5:2, v/v/v/v). The flow rate of the mobile phase was set at 1.5 mL/min and the column temperature was set at 30 °C.

2.7. Determination of dopamine and serotonin concentrations by HPLC–ECD

Dopamine and serotonin levels in the rat striatum were determined by HPLC using an HTEC-500 system (Eicom, Kyoto) equipped with ECD. Samples (10 μL) were injected and analytes were separated on an Eicompak PP-ODS II column (30 × 4.6 mm, i.d., 2 μm, Eicom) using a mixture of 0.1 M phosphate buffer (pH 5.4)/methanol (=98.5:1.5, v/v) containing 500 mg/L sodium 1-decanesulfonate and 50 mg/L EDTA·2Na. The flow rate of the mobile phase was set at 0.5 mL/min and the column temperature was set at 25 °C. The working electrode was a WE-3G (graphite electrode, Eicom). The applied voltage of the conditioning cell was set at +400 mV.

2.8. Determination of drug and monoamines concentrations

MDMA and methamphetamine levels in dialysate were determined from calibration curves ranging from 2.50 to 1000 ng/mL. MDA and amphetamine levels in dialysate were determined from calibration curves ranging from 2.50 to 500 ng/mL. The limits of detection for MDMA, MDA, methamphetamine, and amphetamine were 1.63 ng/mL, 1.19 ng/mL, 1.84 ng/mL, and 0.47 ng/mL, respectively.

Dopamine and serotonin levels in dialysates were also determined from calibration curves ranging from 0.05 nM to 500 nM. The limits of detection for dopamine and serotonin were 0.008 nM and 0.006 nM, respectively.

2.9. Statistical analysis

The concentrations of drugs and monoamines measured in dialysates were converted into extracellular concentrations using *in vivo* recovery. These values were used to obtain the PK parameters of these compounds.

All data are represented as mean ± standard deviation of mean (SD). PK parameters were calculated by moment analysis (Yamaoka et al., 1987). Peak concentration (C_{max}) and time to peak concentration (T_{max}) were obtained from observed data. The area under the curve (AUC) for concentration vs. time was calculated using the linear trapezoidal rule until 600 min after drug administration (AUC_{0-600}). The mean residence time (MRT_{0-600}) was calculated from the equation for area under the moment curve/AUC_{0-600}.

The moment parameters of drugs and monoamines were analyzed by one-way analysis of variance (ANOVA) followed by Scheffe's post-test for more than three groups, and by Student's *t*-test for two groups. A *P*-value less than 0.05 was considered to be statistically significant. Statistical calculations were performed using IBM SPSS® Statistics 17.0 (SPSS Japan Inc., Tokyo).

3. Results

3.1. Determination of drug profiles in dialysates

3.1.1. Monitoring of MDMA and MDA levels in the rat brain after sole administration of MDMA and co-administration of MDMA with methamphetamine

The profiles of extracellular MDMA and MDA concentrations vs. time after i.p. administration of MDMA alone (12 and 25 mg/kg) and co-administration of MDMA (12 mg/kg) and

methamphetamine (10 mg/kg) are shown in Fig. 1. Moment parameters for these experiments are shown in Table 1.

When MDMA was administered alone, extracellular C_{max} and AUC_{0-600} of MDMA were significantly increased for 25 mg/kg vs. 12 mg/kg (extracellular C_{max} 1847.9 to 6077.7 ng/mL; AUC_{0-600} 348.0 μg min/L to 1490.9 μg min/L; $P = 0.01$ for both, Scheffe's post-hoc test). Moreover, C_{max} of MDMA for the co-administration group was 3308.1 ng/mL; a non-significant increase compared with the sole MDMA (12 mg/kg) group. After sole administration of MDMA (12 and 25 mg/kg), C_{max} of MDA was 327.1 ng/mL and 1351.9 ng/mL, respectively, and AUC_{0-600} of MDA was 107.9 μg min/L and 483.4 μg min/L, respectively. This represented a non-significant increase in MDA levels in the 25 mg/kg MDMA group compared with those in the 12 mg/kg group.

3.1.2. Monitoring of methamphetamine and amphetamine levels in the rat brain after sole administration of methamphetamine and co-administration of MDMA and methamphetamine

The profiles of extracellular methamphetamine and amphetamine concentrations vs. time after i.p. administration of methamphetamine alone (10 mg/kg) and co-administration of MDMA (12 mg/kg) and methamphetamine (10 mg/kg) are shown in Fig. 2. Moment parameters for these experiments are shown in Table 2.

The C_{max} of methamphetamine did not differ significantly between the sole methamphetamine administration and MDMA-methamphetamine co-administration groups (2757.1 ng/mL vs. 2675.1 ng/mL). However, the T_{max} of methamphetamine was significantly prolonged in the co-administration group compared with the sole MP group (45.0 min to 110.0 min, $P = 0.01$, Student's *t*-test). In addition, in the co-administration group, the MRT_{0-600} of methamphetamine was significantly prolonged from 123.0 min to 210.3 min when compared with the sole methamphetamine group ($P < 0.05$, Student's *t*-test). The AUC_{0-600} of methamphetamine showed a non-significant tendency to increase in the co-administration group compared with the sole methamphetamine group (671.7 μg min/L vs. 401.8 μg min/L).

One of the major metabolites of methamphetamine, amphetamine, tended to show similar behavior to methamphetamine. The MRT_{0-600} of amphetamine was significantly prolonged in the co-administration group compared with the sole methamphetamine group (187.4 min to 301.4 min; $P = 0.001$, Student's *t*-test). The C_{max} of amphetamine increased significantly in the co-administration group compared with the sole methamphetamine group (580.5 ng/mL vs. 452.0 ng/mL; $P < 0.05$, Student's *t*-test), as did the AUC_{0-600} of amphetamine (217.4 μg min/L vs. 98.2 μg min/L; $P < 0.05$, Student's *t*-test).

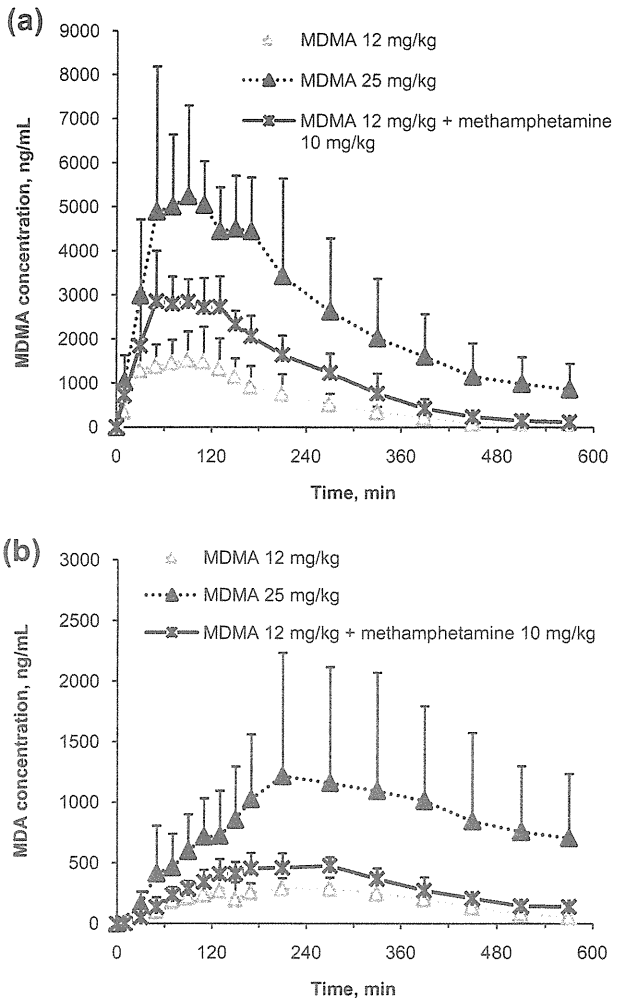

Fig. 1. Time-concentration profiles of extracellular 3,4-methylenedioxymethamphetamine (MDMA) (a) and 3,4-methylenedioxyamphetamine (MDA) (b) after sole administration of MDMA (12 and 25 mg/kg, i.p.) and co-administration of MDMA (12 mg/kg, i.p.) and methamphetamine (10 mg/kg, i.p.) as determined by microdialysis in ethylcarbamate-anesthetized rats Each point represents the mean + standard deviation of mean (SD) ($n = 4$).

Table 1
Pharmacokinetic parameters of 3,4-methylenedioxymethamphetamine (MDMA) and 3,4-methylenedioxyamphetamine (MDA) after a sole administration of MDMA (12 and 25 mg/kg, *i.p.*) and co-administration of MDMA (12 mg/kg, *i.p.*) with methamphetamine (10 mg/kg, *i.p.*).

	MDMA 12 mg/kg	MDMA 25 mg/kg	MDMA 12 mg/kg + methamphetamine 10 mg/kg
MDMA			
C_{max} (ng/mL)	1847.9 ± 599.8	6077.7 ± 2484.1*	3308.1 ± 674.2
T_{max} (min)	85.0 ± 55.1	85.0 ± 30.0	95.0 ± 44.3
$T_{1/2}$ (min)	84.6 ± 12.1	175.4 ± 73.1	96.7 ± 27.3
AUC_{0-600} (μg min/L)	348.0 ± 120.3	1490.9 ± 657.4*	689.8 ± 129.4
MRT_{0-600} (min)	170.9 ± 31.7	205.2 ± 39.9	171.3 ± 32.6
CL (mL/min)	11.0 ± 3.0	5.6 ± 2.3*	5.3 ± 0.9*
MDA			
C_{max} (ng/mL)	327.1 ± 63.5	1351.9 ± 936.1	492.7 ± 90.2
T_{max} (min)	205.0 ± 79.0	290.0 ± 116.6	230.0 ± 49.0
$T_{1/2}$ (min)	150.2 ± 79.0	503.5 ± 309.2	182.5 ± 111.7
AUC_{0-600} (μg min/L)	107.9 ± 27.7	483.4 ± 360.2	166.6 ± 31.9
MRT_{0-600} (min)	258.5 ± 26.9	300.2 ± 32.7	271.9 ± 16.9

Data were represented as mean ± standard deviation of mean (SD).
P-values were calculated by Scheffe's post-hoc test for the three groups.
* $P < 0.05$, vs. MDMA (12 mg/kg) group (Scheffe's post-hoc test).

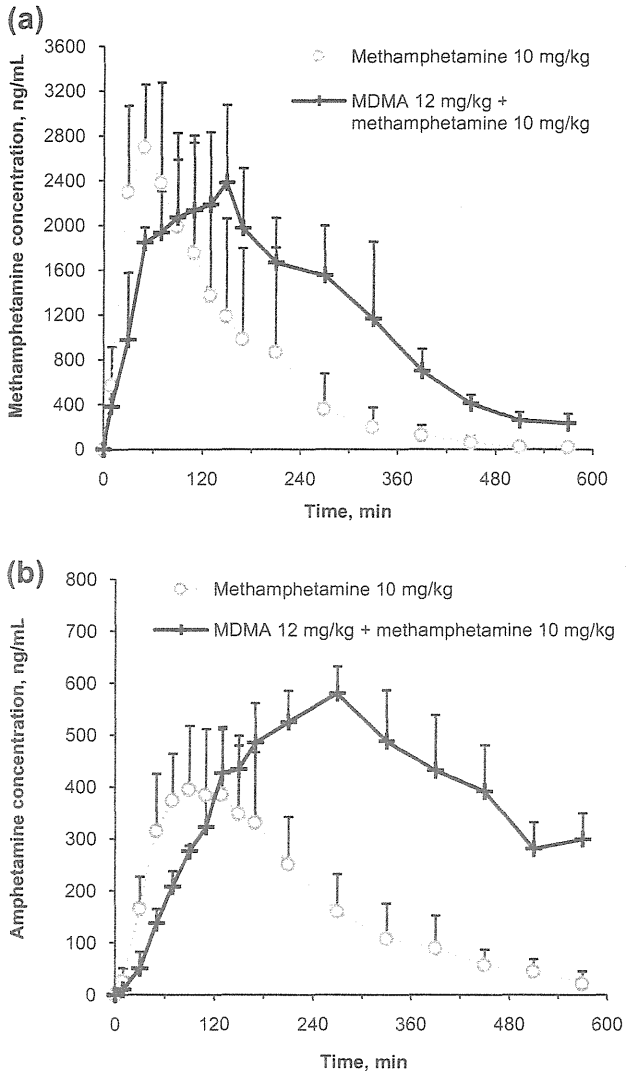

Fig. 2. Time-concentration profiles of extracellular methamphetamine (a) and amphetamine (b) after sole administration of methamphetamine (10 mg/kg, i.p.) and co-administration of 3,4-methylenedioxymethamphetamine (MDMA) (12 mg/kg, i.p.) and methamphetamine (10 mg/kg, i.p.) as determined by microdialysis in ethylcarbamate-anesthetized rats Each point represents the mean + standard deviation of mean (SD) ($n = 4$).

3.2. Determination of monoamine profiles in dialysates

3.2.1. Effects of MDMA with/without methamphetamine on dopamine and serotonin levels in the rat brain

The profiles of extracellular dopamine and serotonin concentrations vs. time after i.p. administration of MDMA alone (12 and 25 mg/kg), methamphetamine (10 mg/kg) alone or co-administration of MDMA (12 mg/kg) with methamphetamine (10 mg/kg) are shown in Fig. 3. Moment parameters for these experiments are shown in Table 3.

The C_{max} of dopamine increased in a dose-dependent manner after sole administration of MDMA (12 mg/kg, 196.8 nM; 25 mg/kg, 882.1 nM). The AUC_{0-600} of dopamine after sole administration of MDMA was 29.9 μM min for 12 mg/kg and 123.4 μM min for 25 mg/kg. The C_{max} of dopamine for the sole methamphetamine administration group was 1687.3 nM, significantly higher than that in the sole MDMA (12 mg/kg) administration group ($P < 0.05$, Scheffe's post-hoc test). The AUC_{0-600} of dopamine after sole administration of methamphetamine was significantly higher than that after sole administration of MDMA (12 mg/kg) (159.9 μM min vs. 29.9 μM min; $P < 0.05$, Scheffe's post-hoc test). Further, the AUC_{0-600} of dopamine in the co-administration group was significantly increased compared with both sole MDMA administration groups (243.4 μM min vs. 29.9 μM min (12 mg/kg MDMA) and 123.4 μM min (25 mg/kg MDMA); $P < 0.05$ for both, Scheffe's post-hoc test).

On the other hand, the C_{max} of serotonin after co-administration of MDMA and methamphetamine tended to be higher than in the sole administration groups (183.3 nM vs. 50.7 nM (MDMA 12 mg/kg), 43.2 nM (MDMA 25 mg/kg) and 36.9 nM (methamphetamine 10 mg/kg); $P > 0.05$, Scheffe's post-hoc test). AUC_{0-600} of serotonin tended to be highest in the co-administration group compared with the sole administration groups (11.4 μM min vs. 4.9 μM min (MDMA 12 mg/kg); 6.1 μM min (MDMA 25 mg/kg), and 2.6 μM min (methamphetamine 10 mg/kg)).

Table 2
Pharmacokinetic parameters of methamphetamine and amphetamine after a sole administration of methamphetamine (10 mg/kg, *i.p.*) with/without 3,4-methylenedioxymethamphetamine (MDMA) (12 mg/kg, *i.p.*).

	MP 10 mg/kg	MDMA 12 mg/kg + methamphetamine 10 mg/kg
Methamphetamine		
C_{max} (ng/mL)	2757.1 ± 626.0	2675.1 ± 594.3
T_{max} (min)	45.0 ± 10.0	110.0 ± 36.5[a]
$T_{1/2}$ (min)	70.4 ± 20.8	117.6 ± 34.6
AUC_{0-600} (μg min/L)	401.8 ± 213.6	671.7 ± 151.2
MRT_{0-600} (min)	123.0 ± 17.4	210.3 ± 6.5[a]
CL (mL/min)	8.8 ± 4.0	4.6 ± 1.1
Amphetamine		
C_{max} (ng/mL)	452.0 ± 81.8	580.5 ± 51.2[a]
T_{max} (min)	115.0 ± 44.3	270.0 ± 0.0
$T_{1/2}$ (min)	109.3 ± 32.3	309.0 ± 143.8[a]
AUC_{0-600} (μg min/L)	98.2 ± 23.3	217.4 ± 27.4[a]
MRT_{0-600} (min)	187.4 ± 34.2	301.4 ± 7.2[a]

Data were represented as mean ± standard deviation of mean (SD).
P-values were calculated by Student's *t*-test for the two groups.
[a] $P < 0.05$, vs. methamphetamine (10 mg/kg) group (Student's *t*-test).

4. Discussion

Hyperthermia is a potentially lethal adverse reaction to MDMA abuse (Greene et al., 2003; Sano et al., 2009), and its underlying mechanism is thought to involve changes in monoamine levels (Mechan et al., 2002; Cole and Sumnall, 2003; Lyles and Cadet, 2003; Docherty and Green, 2010). Therefore monitoring of brain monoamine levels should be useful in evaluating the risks of MDMA.

We investigated pharmacokinetic and pharmacodynamic effects of the drugs simultaneously for each rat striatum. First, we investigated pharmacokinetic and pharmacodynamic profiles of MDMA at two dosages, 12 mg/kg and 25 mg/kg. Because seized MDMA tablets are known to range widely in MDMA content, it is important to evaluate the *in-vivo* effect of MDMA at different doses. Second, to clarify the risks of abusing both MDMA with methamphetamine concurrently, we also evaluated pharmacokinetic and pharmacodynamic profiles in the rat striatum associated with co-administration of the two drugs. To our knowledge, this is the first study that has taken into account interactions of MDMA with methamphetamine when evaluating pharmacokinetics and pharmacodynamics based on

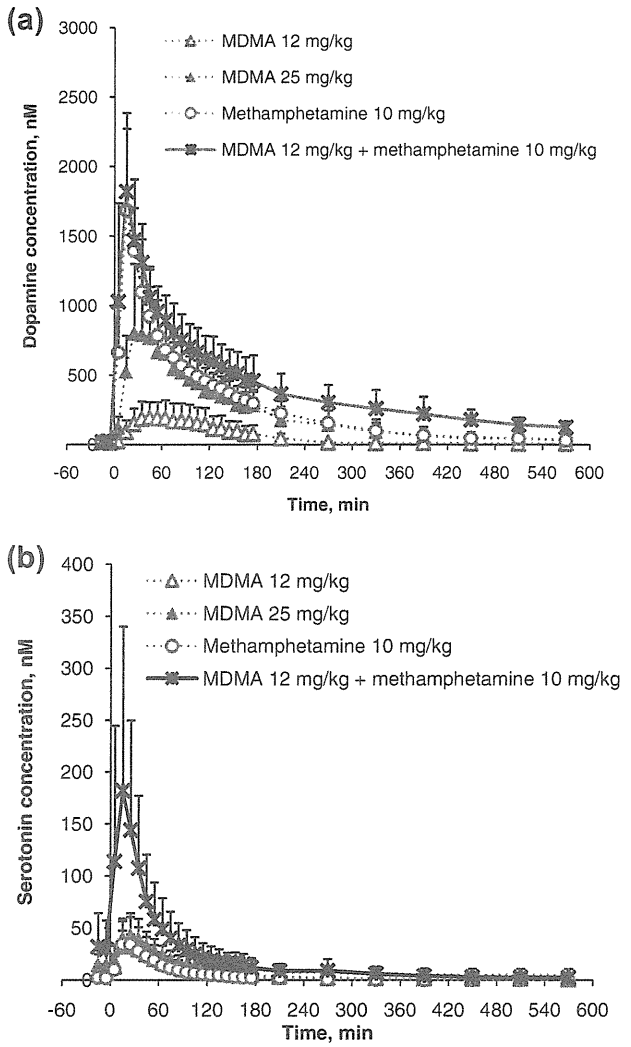

Fig. 3. Time-concentration profiles of extracellular dopamine (a) and serotonin (b) after sole administration of 3,4-methylenedioxymethamphetamine (MDMA) (12 and 25 mg/kg, i.p.) or methamphetamine (10 mg/kg, i.p.) and co-administration of MDMA (12 mg/kg, i.p.) with methamphetamine (10 mg/kg, i.p.) as determined by microdialysis in ethylcarbamate-anesthetized rats Each point represents the mean + standard deviation of mean (SD) ($n = 4$).

the monitoring of drugs, metabolites, and monoamine levels in the rat striatum over time.

In the pharmacokinetic evaluation, C_{max} and AUC_{0-600} of MDMA after a sole administration of 25 mg/kg MDMA were significantly increased compared with those for 12 mg/kg MDMA. This indicates that MDMA ingestion influenced the brain in a dose-dependent manner. Although the higher MDMA dose was approximately twice the lower dose, these pharmacokinetic changes were greater than anticipated from the dose difference. This results support the hypothesis that MDMA shows a non-linear accumulation (Chu et al., 1996; la de Torre et al., 2000; Kolbrich et al., 2008; Mueller et al., 2008).

In the sole 25 mg/kg MDMA administration group, CL of MDMA was significantly diminished compared with the sole 12 mg/kg MDMA administration group, and leaded to increased AUC_{0-600} of MDMA. Moreover, when 12 mg/kg MDMA was co-administered with 10 mg/kg methamphetamine, C_{max} and AUC_{0-600} of MDMA tended to increase compared with after sole administration of MDMA at the same dose, but this was not significant. Similar to the sole 25 mg/kg administration group, CL of MDMA in co-administration group was significantly diminished compared with the sole 12 mg/kg MDMA administration group. In MDMA metabolism to MDA, no significant change in the pharmacokinetic parameters of MDA was found between a sole 12 mg/kg MDMA administration and co-administration groups. So, the efflux step from the brain thought to be prolonged by drug–drug interaction, and this caused decreased CL of MDMA. Pal and Mitra (2006) suggested that MDMA and amphetamine are potent substrates for P-glycoprotein, an efflux protein, which is located in the brain and transports substrates towards the blood compartment (Cordon-Cardo et al., 1989; Mann et al., 1997). Furthermore, Ketabi-Kiyanvash et al. (2003) indicated MDMA at high concentration acts as an inhibitor on P-glycoprotein. These data suggest saturation of efflux via P-glycoprotein or inhibition of P-glycoprotein could be occurred and leads to decreased CL of MDMA in higher dose of 25 mg/kg MDMA group.

Increased C_{max} of MDMA was observed in co-administration group, whereas C_{max} of methamphetamine did not change between two groups. This may show the possibility of drug–drug interaction between MDMA and methamphetamine in the influx steps into the brain. Unfortunately, the details of influx of amphetamine-like drug into brain have not been elucidated. Further study is needed to be clear disposition of drugs into brain and drug–drug interaction about that.

With regard to methamphetamine, T_{max} and MRT_{0-600} after co-administration of 12 mg/kg MDMA with 10 mg/kg methamphetamine were significantly prolonged compared with after sole administration of the same dose of methamphetamine. These findings indicate that the brain was exposed to methamphetamine for longer when MDMA was taken concurrently than when metham-

Table 3
Moment parameters of dopamine and serotonin levels after a sole administration of 3,4-methylenedioxymethamphetamine (MDMA) (12 and 25 mg/kg, *i.p.*) or methamphetamine (10 mg/kg, *i.p.*) and a co-administration of MDMA (12 mg/kg, *i.p.*) with methamphetamine (10 mg/kg, *i.p.*).

	MDMA 12 mg/kg	MDMA 25 mg/kg	Methamphetamine 10 mg/kg	MDMA 12 mg/kg + methamphetamine 10 mg/kg
Dopamine				
C_{max} (nM)	196.8 ± 100.6	882.1 ± 421.7	1687.3 ± 584.5*	1823.5 ± 560.6*
T_{max} (min)	42.5 ± 20.6	35.0 ± 14.1	15.0 ± 0.0	17.5 ± 5.0
AUC_{0-600} (μM min)	29.9 ± 17.5	123.4 ± 47.3	159.9 ± 50.9*	243.4 ± 65.7*, **
MRT_{0-600} (min)	151.9 ± 41.5	150.4 ± 28.8	123.0 ± 31.4	171.9 ± 27.8
Serotonin				
C_{max} (nM)	50.7 ± 23.8	43.2 ± 17.6	36.9 ± 12.6	183.3 ± 157.2
T_{max} (min)	25.0 ± 8.2	25.0 ± 8.2	22.5 ± 5.0	17.5 ± 5.0
AUC_{0-600} (μM min)	4.9 ± 2.5	6.1 ± 3.2	2.6 ± 1.0	11.4 ± 8.4
MRT_{0-600} (min)	110.4 ± 17.2	164.3 ± 73.4	80.2 ± 16.1	105.9 ± 30.2

Data were represented as mean ± standard deviation of mean (SD).
P-values were calculated by Scheffe's post-hoc test for the four groups.
* $P < 0.05$, vs. MDMA (12 mg/kg) group (Scheffe's post-hoc test).
** $P < 0.05$, vs. MDMA (25 mg/kg) group (Scheffe's post-hoc test).

phetamine was given alone. This may result from interactions at uptake and excretion, but the detailed mechanisms remain unclear.

In the evaluation of pharmacodynamics, we found a significant increase of dopamine concentration after co-administration of MDMA (12 mg/kg) with methamphetamine (10 mg/kg) compared with sole administration of either 12 or 25 mg/kg MDMA. Further, we found that methamphetamine contributed to this increase in dopamine concentration more than did MDMA when the two drugs were co-administered. This suggests that adverse events would be more common when MDMA is taken with methamphetamine than when it is ingested by itself, even at twice the dose. Serotonin concentration also tended to increase when MDMA and methamphetamine were given together. This may be another factor increasing the risk of MDMA when ingested with methamphetamine.

As above, C_{max} and AUC_{0-600} of serotonin tended to increase after co-administration of MDMA with methamphetamine, although not significantly when compared with the sole administration groups. A relatively large variation in these serotonin parameters may account for this failure of the differences to reach significance, and this could be caused by individual differences in drug sensitivity among rats. Nonetheless, this finding still indicates that serotonin release is increased by taking MDMA with methamphetamine, and that such co-ingestion accordingly increases the risks of these drugs.

Our findings agree with those of Clemens et al. (2004, 2005), who reported that MDMA and methamphetamine in combination may have greater acute adverse effects than equivalent doses of either drug alone. Gouzoulis-Mayfrank and Daumann (2009) also suggested that multi-drug use may well potentiate the neurotoxic effects of the drugs, and our present findings are again in line with this report.

We could control for the differences between individual rats and discuss the relationships between drugs and monoamines levels in the rat brain because pharmacokinetic and pharmacodynamic evaluations were performed the using same sample for each individual. Regarding the pharmacokinetic assessment, there was no significant difference in the changes in MRT_{0-600} between drugs and monoamines (data not shown). This suggests that monoamine profiles directly reflect the pharmacokinetics of drugs distributed to the brain, indicating that monoamines are released in response to the drug entering the brain.

Finally, we need to refer to several limitations in this study. First, two different doses were used in this study, although several doses were required to evaluate toxicity of MDMA. Second, our results obtained by single administration of drugs indicated acute effects of drugs. Their chronic effects by multiple administrations should be also considered. So, we need further study to overcome these limitations.

5. Conclusion

In conclusion, we compared pharmacokinetic and pharmacodynamic profiles for sole administration of MDMA (12 and 25 mg/kg), sole administration of methamphetamine (10 mg/kg), and co-administration of MDMA (12 mg/kg) with methamphetamine (10 mg/kg). Our findings suggest that the risks of MDMA ingestion may be increased by co-administration of methamphetamine.

References

Chu, T., Kumagai, Y., DiStefano, E.W., Cho, A.K., 1996. Disposition of methylenedioxymethamphetamine and three metabolites in the brains of different rat strains and their possible roles in acute serotonin depletion. Biochem. Pharmacol. 51, 789–796.

Clemens, K.J., van Nieuwenhuyzen, P.S., Li, K.M., Cornish, J.L., Hunt, G.E., McGregor, I.S., 2004. MDMA ("ecstasy"), methamphetamine and their combination: long-term changes in social interaction and neurochemistry in the rat. Psychopharmacology 173, 318–325.

Clemens, K.J., Cornish, J.L., Li, K.M., Hunt, G.E., McGregor, I.S., 2005. MDMA ("ecstasy"), methamphetamine and their combination: order of administration influences hyperthermic and long-term adverse effects in female rats. Neuropharmacol 49, 195–207.

Cole, J.C., Sumnall, H.R., 2003. The pre-clinical behavioural pharmacology of 3,4-methylenedioxymethamphetamine (MDMA). Neurosci. Biobehav. Rev. 27, 199–217.

Cordon-Cardo, C., O'Brien, J.P., Casals, D., Rittman-Grauer, L., Biedler, J.L., Melamed, M.R., Bertino, J.R., 1989. Multidrug-resistance gene (P-glycoprotein) is expressed by endothelial cells at blood-brain barrier sites. Proc. Natl. Acad. Sci. USA 86, 695–698.

Docherty, J.R., Green, A.R., 2010. The role of monoamines in the changes in body temperature induced by 3,4-methylenedioxymethamphetamine (MDMA, ecstasy) and its derivatives. Br. J. Pharmacol. 160, 1029–1044.

Fox, H.C., McLean, A., Turner, J.J.D., Parrott, A.C., Rogers, R., Sahakian, B.J., 2002. Neuropsychological evidence of a relatively selective profile of temporal dysfunction in drug-free MDMA ("ecstasy") polydrug users. Psychopharmacology 162, 203–214.

Gouzoulis-Mayfrank, E., Daumann, J., 2009. Neurotoxicity of drug of abuse-the case of methylenedioxyamphetamine (MDMA, ecstasy), and amphetamines. Dialogues Clin. Neurosci. 11, 305–317.

Greene, S.L., Dargan, P.I., O'connor, N., Jones, A.L., Kerins, M., 2003. Multiple toxicity from 3,4-methylenedioxymethamphetamine ("Ecstasy"). Am. J. Emerg. Med. 21, 121–124.

Hall, A.P., Henry, J.A., 2006. Acute toxic effects of 'Ecstasy' (MDMA) and related compounds: overview of pathophysiology and clinical management. Br. J. Anaesth. 96, 678–685.

Han, D.D., Gu, H.H., 2006. Comparison of the monoamine transporters from human and mouse in there sensitivities to psychostimulant drugs. BMC Pharmacol. 6, 6–12.

Ikeda, R., Igari, Y., Fuchigami, Y., Wada, M., Kuroda, N., Nakashima, K., 2011. Pharmacodynamic interactions between MDMA and concomitants in MDMA tablets on extracellular dopamine and serotonin in the rat brain. Eur. J. Pharmacol. 660, 318–325.

Irvine, R.J., Keane, M., Felgate, P., McCann, U.D., Callaghan, P.D., White, J.M., 2001. Plasma drug concentrations and physiological measures in 'dance party' participants. Neuropsychopharmacol. 31, 424–430.

Kaye, S., Darke, S., Duflou, J., 2009. Methylenedioxymethamphetamine (MDMA)-related fetelities in Australia: demographics, circumstances, toxicology and major organ pathology. Drug Alchol Depend. 104, 254–261.

Ketabi-Kiyanvash, N., Weiss, J., Haefeli, W.E., Mikus, G., 2003. P-glycoprotein modulation by the designer drugs methylenedioxymethamphetamine, methylenedioxyethylamphetamine and paramethoxyamphetamine. Addict. Biol. 8, 413–418.

Kolbrich, E.A., Goodwin, R.S., Gorelick, D.A., Hayes, R.J., Stein, E.A., Huestis, M.A., 2008. Plasma pharmacokinetics of 3,4-methylenedioxymethamphetamine after controlled oral administration to young adults. Ther. Drug Monit. 30, 320–332.

la de Torre, R., Farre, M., Ortuno, J., Mas, S., Brennieisen, R., Roset, P.N., Segura, J., Cami, J., 2000. Non-linear pharmacokinetics of MDMA ('ecstasy') in humans. Br. J. Clin. Pharmacol. 49, 104–109.

Lyles, J., Cadet, J.L., 2003. Methylenedioxymethamphetamine (MDMA, Ecstasy) neurotoxicity: cellular and molecular mechanisms. Brain Res. Rev. 42, 155–168.

Makino, Y., Tanaka, S., Kurobane, S., Nakauchi, M., Terasaki, T., Ohta, S., 2003. Profiling of illegal amphetamine-type stimulant tablets in Japan. J. Health Sci. 49, 129–137.

Mann, H., Ladenheim, B., Hirata, H., Moran, T.H., Cadet, J.L., 1997. Differential toxic effects of methamphetamine (METH) and methylenedioxymethamphetamine (MDMA) in multidrug-resistant (mdr 1a) knockout mice. Brain Res. 769, 340–346.

McCann, U.D., Ricaurte, G.A., 2001. Caveat emptor: editors beware. Neuropsychopharmacology 24, 333–334.

Mechan, A.O., Esteban, B., O'Shea, E., Elliott, J.M., Colado, M.I., Green, A.R., 2002. The pharmacology of the acute hyperthermic response that follows administration of 3,4-methylenedioxymethamphetamine (MDMA, 'ecstasy') to rats. Br. J. Pharmacol. 135, 170–180.

Morefield, K.M., Keane, M., Felgate, P., White, J.M., Irvine, R.J., 2011. Pill content, dose and resulting plasma concentrations of 3,4-methylenedioxymethamphetamine (MDMA) in recreational 'ecstasy' users. Addiction 106, 1293–1300.

Mueller, M., Peters, F.T., Maurer, H.H., McCann, U.D., Ricaurte, G.A., 2008. Nonlinear pharmacokinetics of (±)3,4-methylenedioxymethamphetamine (MDMA, "Ecstasy") and its major metabolites in squirrel monkeys at plasma concentrations of MDMA that develop after typical psychoactive doses. J. Pharmacol. Exp. Ther. 327, 38–44.

Nakashima, K., Yamasaki, H., Kuroda, N., Akiyama, S., 1995. Evaluation of lophine derivatives as chemiluminogens by a flow-injection method. Anal. Chim. Acta 303, 103–108.

National Police Agency of Japan., 2011. The White Paper on POLICE 2011. National Police Agency, Tokyo, Japan.

National Institute on Drug Abuse (NIDA), 2006a. Research Report Series MDMA(ECSTASY). NIH, Publication Number 06-4728.

National Institute on Drug Abuse (NIDA), 2006b. Research Report Series METHAMPHETAMINE. NIH, Publication Number 06-4210.

Numachi, Y., Ohara, A., Yamashita, M., Fukushima, S., Kobayashi, H., Hata, H., Watanabe, H., Hall, F.S., Lesch, K.P., Murphy, D.L., Uhl, G.R., Sora, I., 2007.

Methamphetamine-induced hyperthermia and lethal toxicity: role of the dopamine and serotonin transporters. Eur. J. Pharmacol. 572, 120–128.
Pal, D., Mitra, A.K., 2006. MDR- and CYP3A4-mediated drug–drug interactions. J. Neuroimmune Pharmacol. 1, 323–339.
Paxinos, G., Watson, G., 2007. The Rat Brain in Stereotaxic Coordinates, fifth ed. Academic Press, California.
Quinton, M.S., Yamamoto, B.K., 2006. Causes and consequences of methamphetamine and MDMA toxicity. AAPS J. 8, E337–347.
Sano, R., Hasuike, T., Nakano, M., Kominato, Y., Itoh, H., 2009. A fatal case of myocardial damage due to misuse of the "designer drug" MDMA. Leg. Med. 11, 294–297.
Silins, E., Copeland, J., Dillon, P., 2009. Patterns and harms of pharmaceutical drug use among ecstasy users in Australia. Adicciones 21, 347–362.
Sun, Y., Nakashima, M.N., Takahara, M., Kuroda, N., Nakashima, K., 2002. Determination of bisphenol A in rat brain by microdialysis and column switching high-performance liquid chromatography with fluorescence detection. Biomed. Chromatogr. 16, 319–326.
Teng, F., Wu, S., Liu, C., Li, J., Chien, C., 2006. Characteristics and trends of 3,4-methylenedioxymethamphetamine (MDMA) tablets found in Taiwan from 2002 to February 2005. Forensic Sci. Int. 161, 202–208.
The PubChem Project: <http://pubchem.ncbi.nlm.nih.gov> (accessed 19.12.12).
Tohmas, D.M., Perez, M.A., Francescutti-Verbeem, D.M., Shah, M.M., Kuhn, D.M., 2010. The role of endogenous serotonin in methamphetamine-induced neurotoxicity to dopamine nerve endings of the striatum. J. Neurochem. 115, 595–605.
Tomita, M., Nakashima, N.M., Wada, M., Nakashima, K., 2007. Sensitive determination of MDMA and its metabolite MDA in rat blood and brain microdialysates by HPLC with fluorescence detection. Biomed. Chromatogr. 21, 1016–1022.
Verheyden, S.L., Henry, J.A., Curran, V.H., 2003. Acute, sub-acute and long-term subjective consequences of 'ecstasy' (MDMA) consumption in 430 regular users. Hum. Psychopharmacol. 18, 507–517.
Wada, M., Yokota, C., Ogata, Y., Kuroda, N., Yamada, H., Nakashima, K., 2008. Sensitive HPLC-fluorescence detection of morphine labeled with DIB-Cl in rat brain and blood microdialysates and its application to the preliminarily study of the pharmacokinetic interaction between morphine and diclofenac. Anal. Bioanal. Chem. 391, 1057–1062.
Yamaoka, K., Nakagawa, T., Uno, T., 1987. Statistical moments in pharmacokinetics. J. Pharmacokinet. Biop. 6, 547–558.

いわゆる“脱法ドラッグ(脱法ハーブ)”による健康被害を防ぐために
～ The researcher consortium that carries the future ～

国立医薬品食品衛生研究所 生薬部第３室 室長　花尻（木倉）瑠理

1. はじめに

近年，“脱法ハーブ”という言葉がしばしば報道に登場するようになった。「脱法ハーブ吸引後に救急搬送」「脱法ハーブを吸って運転し自動車事故」等の文字が紙面を賑わす。当初は“ハーブ”そのものが悪役と誤解され，「そんな危険なハーブが日本に流通しているか？」「脱法ハーブにはどのような植物があるのか？」等の問い合わせを多数いただいた。しかし，この“脱法ハーブ”と呼ばれる製品の実態は，乾燥した植物細片に麻薬様の強い作用を有する化学合成化合物を添加したものであり，主にお香やタバコのように煙を吸引して使用される。製品に使用されている植物自体は，西洋ではお茶などに使用されるふつうの“ハーブ”であることが多い。

国立医薬品食品衛生研究所（国立衛研）生薬部第３室では，いわゆる薬物４法で厳しく規制される覚せい剤，麻薬，大麻，あへん，また薬事法下で流通が規制される指定薬物や無承認無許可医薬品などを対象とした試験研究を業務としている。“脱法ハーブ”と呼ばれる形態の製品が日本で本格的に流通し始めたのは2008年前後であるが，それ以前から“合法ドラッグ”“脱法ドラッグ”と呼ばれる様々な化学物質や植物が法律の規制枠を逃れて販売，乱用され，大きな問題となっていた。和漢薬の内容からは外れてしまうが，本稿では，我々国立衛研生薬部第３室の“脱法ドラッグ（脱法ハーブ）”への取り組みを中心に，この10年間の“脱法ドラッグ”流通と国の監視指導行政の移り変わりについて紹介したい。

2. “脱法ドラッグ”と指定薬物制度

“脱法ドラッグ”（公的には“違法ドラッグ”。以下，違法ドラッグと記載）とは，一般に，麻薬及び向精神薬取締法上の「麻薬」または「向精神薬」には指定されていないが，それらと類似の有害性を有することが疑われる物質（人為的に合成されたもの，天然物及びそれに由来するものを含む）であり，もっぱら人の乱用に供することを目的として製造，販売等されるものを示す。比較的安価で，繁華街の路上やアダルトショップ，インターネットなどで容易に入手が可能であったことから，2000年前後より特に青少年の間で蔓延し，健康被害や社会的弊害が大きな問題となった。深刻化する違法ドラッグ問題に対応するため，厚生労働省は2006年に薬事法を改正し，興奮等の作用を有する可能性が高く，保健衛生上の危害が発生する恐れがある薬物や植物を厚生労働大臣が「指定薬物」として指定し，医療等の用途以外の製造，輸入，販売等を禁止することとなった。2007年４月に31化合物１植物が最初に指定薬物として規制されて以来，2013年５月末時点で計12回の指定薬物指定が行われ，より規制の厳しい麻薬に指定された15化合物を除き，875化合物１植物（うち包括指定772化合物）が指定薬物として規制されている（図1）。

国立衛研生薬部第３室では，業務の一部として，指定薬物制度に対応し，問題となる化合物や植物の規制化に必要な評価手法及び科学的データを監視指導・麻薬行政に提供することを目的とした試験研究を行っている。特に，違法ドラッグ製品の流通実態を把握することを目的とし，2002年度より，厚生労働省が全国都道府県に委託して買い上げた違法ドラッグ製品及び国立衛研が独自に行っているインターネット等買上違法ドラッグ製品の含有成分分析調査を実施している。2012年度までに国立衛研が調査した違法ドラッグ製品は総計2200製品以上にもおよぶ。参考として，2002年度から2011年度の10年間で厚生労働省が全国都道府県に委託して買い上げた違法ドラッグ691製品において，違法ドラッグ成分が検出された製品数（のべ数）の移り変わりを図２に記載した。

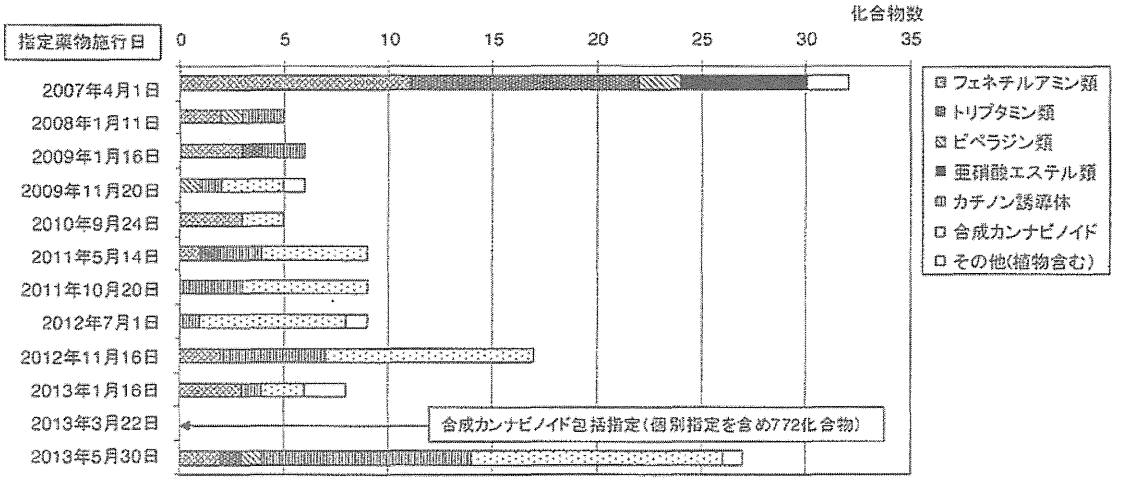

図1　指定薬物として規制された化合物の種類と数

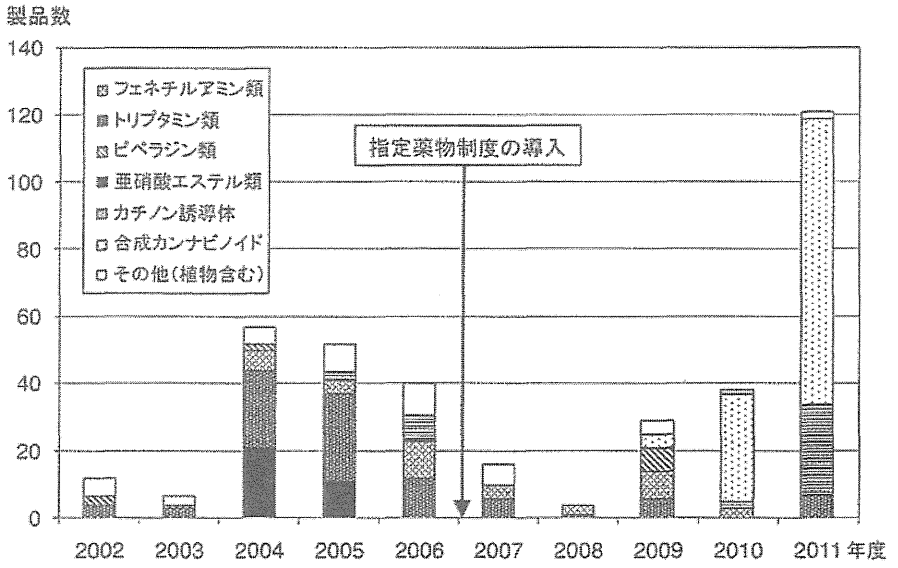

図2　2002年度から2011年度の10年間で厚生労働省全国買い上げ製品において違法ドラッグ成分が検出された製品数（のべ数）の移り変わり（参考文献1より一部抜粋）

我々の分析調査結果[1),3)]では，指定薬物制度制定前に流通していた違法ドラッグの主流は*Salvia divinorum*等の幻覚成分を含む植物，5-MeO-DIPT（別名Foxy，2005年4月麻薬として規制）等のトリプタミン類，2C-T-7（2006年4月麻薬として規制）等のフェネチルアミン類及びピペラジン類等であった。また，RUSH等の名で知られた亜硝酸エステル類も違法ドラッグとして広く流通した（図3）。これらの化合物が麻薬もしくは指定薬物として規制されるとその流通は激減したが，規制された化合物に代わり，構造類似化合物が市場に出現した。現在では，カチノン誘導体やカンナビノイド受容体作動薬（合成カンナビノイド）が流通の主流となっている。特に，2008年度にその存在が明らかとなった合成カンナビノイドが添加された植物製品（"Spice"の名称で世界的に広く流通，図4）の登場は，従来の違法ドラッグの概念を大きく変えた。合成カンナビノイドは，医薬品開発途上でメディシナルケミストリーによって大量に誕生したカンナビノイド受容体に対し高い活性を有する化合物群である。これら化合物を乾燥植物細片に混合した"脱法ハーブ"製品が，大麻様の作用を標榜して違法ドラッグ市場に次から次へと登場している。同様に，カチノン誘導体やその他化合物についても，アロマリキッドやバスソルト等を標榜して，溶液や粉末状態で，様々な構造類似化合物が違法ドラッグ市場に続々と登場している。これら違法ドラッグについては，指定薬物や麻薬に指定されると同時に構造類似化合物が新たに市場に登場し，規制との「いたちごっこ」が続いている。

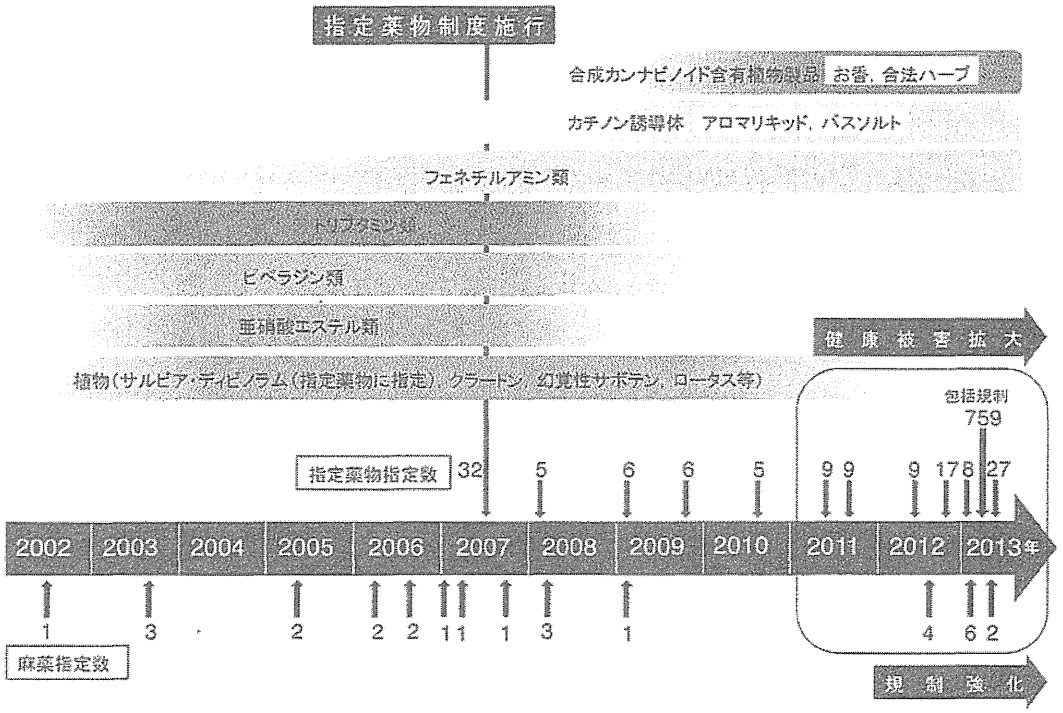

図3 過去10年間における違法ドラッグの流通と規制の移り変わり

図4 いわゆる"脱法ハーブ"の元祖"Spice"製品シリーズ

なお,"脱法ハーブ"に使用されている植物についての情報は極めて乏しい。我々は,合成カンナビノイドを含有する"脱法ハーブ"製品について,含有植物細片の遺伝子分析を行い,使用されている植物の基原種調査を行った[4]。その結果,含有植物は製品の包装に表示されていた植物名とは異なり,大麻や*Salvia divinorum*, Kratom等,実際に活性成分を含有する植物も数製品から検出されたが,ほとんどの製品では向精神活性が報告されている植物は認められなかった。

3."脱法ハーブ"の流通と包括規制

2012年以降,違法ドラッグが関与したと考えられる救急搬送事例(死亡事例を含む)や自動車事故等の他害事件の報告が著しく増加している。正式には報告されていない事例も含めると,件数はさらに増えるものと考えられる。厚生労働省は規制の「いたちごっこ」的状況を打破すべく,①指定薬物指定の迅速化,②構造類似体を一括して取り締まりの対象に指定する包括指定の導入,等の方針を打ち出した。また,濫用実態や依存性等の中枢毒性が確認された指定薬物については,より厳しい規制区分である麻薬への指定を積極的に行うとした。これをうけて2012年度においては,違法ドラッグの規制化が急速に進み,指定薬物61化合物(うち2化合物はさらに麻薬として指定,27化合物は2013年4

月30日省令公布)，麻薬12化合物（うち2化合物は2013年4月26日政令公布)が新規に指定された。また合成カンナビノイドのうち，ナフトイルインドール骨格に特定の置換基を有する化合物群759化合物（個別指定化合物を除く）が包括的に指定薬物として新たに指定された。包括規制の施行は2013年3月22日であり，施行前後における違法ドラッグの流通変化については今後の検討課題と思われる。しかし，我々の調査では，少なくとも包括範囲が公開され，パブリックコメント募集が始まった2012年11月以降，包括範囲内の新規化合物は市場に登場しておらず，常に流通の主流であったナフトイルインドール骨格を有する合成カンナビノイドの新たな出現はほぼ沈静化したと考えられた。ただし，2012年度以降，従来の流通化合物には見られない様々な構造を有する違法ドラッグが次々と違法ドラッグ市場に登場しており[5)-7)]，その対応が求められている。

国立衛研生薬部第3室では今までに，迅速な取締りを可能とするために，麻薬及び指定薬物について，依頼に応じて公的試験機関に分析用標品及び分析データを交付してきた。しかし上述した通り，2012年度においては包括指定も含め800化合物以上が新たに指定薬物として指定され，今後も新規化合物が次々と追加されていくことが予想される。そのため，個別に対応していた従来の方法では対応しきれなくなっている。特に，規制する化合物の構造を個々には指定しない包括指定においては，未知化合物が検出された場合，その化合物が包括指定範囲に相当するか否かを判断するためには，実際に製品から化合物を精製してその構造を決定する必要が生じる。しかし，NMR等を用いて未知化合物の構造決定を行うことが可能な分析機関は限られている。さらに，未知化合物のみならず構造類似化合物群は，包括規制化合物群も含め，物性や分析データに関する情報が極端に少なく，試薬として入手できないものが多い。このような背景のもと，我々は，2013年度より，違法ドラッグ（未規制・既規制化合物）及びその構造類似化合物等に関する構造情報及び各種分析データ，違法ドラッグ成分を含有する製品情報，分析用標品情報など，科学的データを統括したデータベースを構築するプロジェクトに着手した。2013年度内の試験的な公開をめざして，現在作業を進めている。

4. "脱法ドラッグ" の今後

重ねて言うが，"脱法ハーブ" と呼ばれる植物製品の正体は，中枢薬理活性の強い合成化合物である。"ハーブ" など正規の植物製品を取り扱う業者には，いささか迷惑な話である。本稿においては個々の違法ドラッグについては言及していないが，もともとは医薬品開発目的として，ある特定の受容体などをターゲットとして数百単位で誕生した化合物群の一部が違法ドラッグ市場に流出したものが多い。従って，規制された化合物に代わって，今後も新たな化合物が次々と出現することが予想される。包括規制も解決策のひとつであるが，規制範囲が狭すぎても規制の有効性が小さく，また広げすぎると鑑定分析の観点から実効的な取締りが困難となるため，検討すべき課題は多い。購入する人がいるから販売する人もいる。まずは "脱法ドラッグ" の危険性に関する正しい知識の普及，また特に青少年が興味本位に "脱法ドラッグ" に手を出さないための取り組みが最も重要なポイントかもしれない。我々も，これら違法ドラッグ含有製品による健康危害を防止するために，今後も継続的に新規違法ドラッグの出現を監視し，迅速な規制化・取締りを行うことが可能となる科学的データを地道に蓄積していきたいと考えている。

最後になりましたが，執筆の機会をいただきました独立行政法人医薬基盤研究所薬用植物資源研究センター川原信夫センター長に感謝致します。

5. 参考文献

1) R. Kikura-Hanajiri, N. Uchiyama, M. Kawamura and Y. Goda, Yakugaku Zasshi, 133, 31-40 (2013) [Review].
2) R. Kikura-Hanajiri, N. Uchiyama, M. Kawamura and Y. Goda, Forensic Toxicol., 31, 44-53 (2013).
3) R. Kikura-Hanajiri, N. Uchiyama and Y. Goda, Legal Medicine, 13(3), 109-115 (2011) [Review].
4) J. Ogata, N. Uchiyama, R. Kikura-Hanajiri and Y. Goda, Forensic Sci. Int., 227(1-3), 33-41 (2013).
5) N. Uchiyama, S. Matsuda, M. Kawamura, R. Kikura-Hanajiri and Y. Goda, Forensic Toxicol., doi:10.1007/s11419-013-0182-9.
6) N. Uchiyama, M. Kawamura, R. Kikura-Hanajiri and Y. Goda, Forensic Sci. In,. 227(1-3), 21-32 (2013).
7) N. Uchiyama, S. Matsuda, D. Wakana, R. Kikura-Hanajiri and Y. Goda, Forensic Toxicol., 31, 93-100 (2013).

次回は，国立医薬品食品衛生研究所生薬部の桑田幸恵先生から寄稿していただく予定です。

違法ドラッグ（脱法ドラッグ）の正体は？
～ The researcher consortium that carries the future ～

国立医薬品食品衛生研究所　生薬部第３室　主任研究官　内山奈穂子

１．はじめに

本稿は，2013 年 6 月号（和漢薬 No.721）掲載の「いわゆる “脱法ドラッグ（脱法ハーブ）” による健康被害を防ぐために：花尻（木倉）瑠理」[1] に関連した内容である。花尻[1] が示した通り，近年，いわゆる脱法ハーブなどを含めた脱法ドラッグ（公的には，違法ドラッグ。以後，違法ドラッグと記載）の乱用が問題となっており，これら違法ドラッグの摂取が原因と考えられる救急搬送事例や自動車事故等が多発している。その概要および現状，またこれらに関連した我々国立衛研生薬部第３室の違法ドラッグへの取り組みについては前報[1] の通りであるが，本稿では，違法ドラッグの正体，つまり違法ドラッグ製品中に何が含まれているかについて紹介する。

２．違法ドラッグ（脱法ドラッグ）の正体は？

2008 年辺りから日本国内において，それまで違法ドラッグ市場で主流であった “*Salvia divinorum*” などの幻覚性植物に替わり，いわゆる “Spice” などと呼ばれる植物系違法ドラッグ（脱法ハーブ）製品が広く流通するようになった。2009 年初頭，これら違法ドラッグ製品が実は合成化合物をハーブに混入したものであることを，我々やドイツのグループが同時期に初めて明らかにした[2-4]。そして，これら製品の多くに含有していたのが「合成カンナビノイド」と呼ばれる一連の化合物群である（図 1，1 - 23）[2-5]。図 1 に製品中から検出された合成カンナビノイドの一部を示したが，これらの多くは，カンナビノイド受容体作動薬として，大麻の主活性成分かつ麻薬である Δ^9-テトラヒドロカンナビノール（Δ^9-THC，図 1）と同程度またはより強い中枢作用を

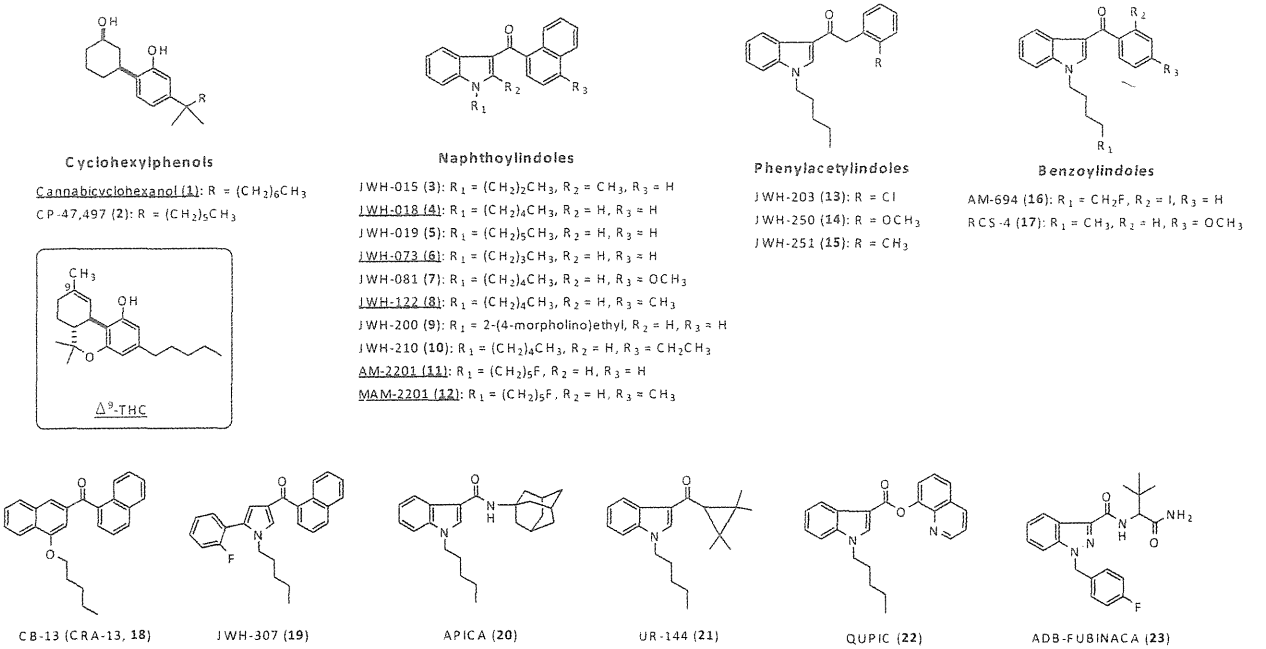

図 1　違法ドラッグ製品から検出された合成カンナビノイドの一部（1 - 23）及び大麻の主活性成分 Δ^9-THC
* 下線化合物：麻薬，その他化合物：指定薬物

有することが報告されている。なお，その他にカチノン系化合物なども製品中から検出されているが，本稿では割愛する[5]。違法ドラッグ製品から初めて検出された合成カンナビノイドは，シクロヘキシルフェノール型のcannabicyclohexanol(1)及びナフトイルインドール型のJWH-018（4）であった（図1）[2-4]。その後，JWH-018（4）の構造類似体（3，5－12）や，フェニルアセチルインドール型（13－15），ベンゾイルインドール型（16，17）合成カンナビノイド，さらに新規骨格を有する合成カンナビノイド（18－23）が次々と検出された（図1）[5]。Cannabicyclohexanol（1）及びCP－47，497（2）はΔ^9－THCの構造類似体であるが，それ以外の化合物（3－23）はΔ^9－THCと全く構造の異なる化合物であった。厚生労働省では，2009年11月以降，これら合成カンナビノイド（1－23を含む）を随時「指定薬物」として規制したが，現在も次々と新規化合物が検出されている。また，2013年6月現在，化合物1，4，6，8，11，12は，「指定薬物」から，より罰則の厳しい「麻薬」に規制されている。

3．では，植物系違法ドラッグ（脱法ハーブ）中のハーブの正体は？

我々はさらに，「脱法ハーブ」に含まれる植物の基原植物種を同定するべく，製品中の植物細片のDNA解析を行った（表1）[6]。その結果，ごく一部の製品で*Salvia divinorum*（指定薬物），Kratom（*Mitragyna speciosa*），大麻（*Cannabis sativa*）などの向精神活性植物が検出されたが，大部分の製品では，西洋でハーブティーなどとして一般的に用いられている植物種（「ハーブ」）が検出された。特に，ダミアナ（Damiana，*Turnera diffusa*）が多くの製品に含まれており，その他に，カンゾウ（Liquorice，*Glycyrrhiza glabra*），チャ（Tea，*Camellia sinensis*），マリーゴールド（Marigold，*Calendula officinalis*），マシュマロウ（Marshmallow，*Althaea officinalis*）など広くハーブとして知られている植物が含まれていた（表1）[6]。従って，製品中の「ハーブ」は，あくまでも活性本体である合成化合物を混入させるための基剤として使用されていると考えられた。

表1　遺伝子解析により植物系違法ドラッグ（脱法ハーブ）製品から同定された植物種のリスト（参考文献6より一部抜粋）

Common name	Plant species
Common balm	*Melissa officinalis*
Damiana	*Turnera diffusa*
Liquorice	*Glycyrrhiza glabra*
Marigold	*Calendula officinalis*
Marshmallow	*Althaea officinalis*
Milkvetch	*Astragalus membranaceus*
Mullein	*Verbascum thapsus*
Raspberry	*Rubus idaeus*
Red Clover	*Trifolium pratense*
Tea	*Camellia sinensis*
Diviner's Sage	*Salvia divinorum*（指定薬物）*
Kratom	*Mitragyna speciosa**
Marijuana/Hemp	*Cannabis sativa*（大麻）*

* 向精神活性植物

4．最後に

日本で厳しく規制されている覚醒剤や麻薬などと比べ，脱法ハーブなどの違法ドラッグ製品はインターネットなどでも簡単に入手できることから，安易に使用する人が増えている。しかし，薬理学的データの乏しいこれら合成化合物を摂取することで，様々な健康被害が生じる可能性が懸念される。従って今後も，継続的な違法ドラッグ製品の流通実態調査を行い，薬物の乱用防止のため，迅速な規制化に貢献するべく努めていきたいと考えている。

今回執筆の機会を頂きました独立行政法人医薬基盤研究所薬用植物資源研究センター長・川原信夫先生に感謝致します。

1）花尻（木倉）瑠理，和漢薬 No.721, 4-7 (2013).
2）N. Uchiyama, R. Kikura-Hanajiri, N. Kawahara, Y. Haishima, Y. Goda, Chem. Pharm. Bull. 57, 439-441 (2009).
3）V. Auwärter , S. Dresen, W. Weinmann , M. Müller , M. Pütz , N. Ferreirós, J. Mass. Spectrom. 44, 832-837 (2009).
4）N. Uchiyama, R. Kikura-Hanajiri, N. Kawahara, Y. Goda, Forensic Toxicol. 27, 61-66 (2009).
5）花尻（木倉）瑠理，内山奈穂子，河村麻衣子，緒方潤，合田幸広，薬学雑誌，133, 31-40 (2013).
6）J. Ogata, N. Uchiyama, R. Kikura-Hanajiri, Y. Goda. Forensic Sci. Int., 227, 33–41 (2013).

次回は，国立医薬品食品衛生研究所食品添加物部の杉本直樹先生から寄稿していただく予定です。

Contents lists available at ScienceDirect

Forensic Science International

journal homepage: www.elsevier.com/locate/forsciint

Characterization of four new designer drugs, 5-chloro-NNEI, NNEI indazole analog, α-PHPP and α-POP, with 11 newly distributed designer drugs in illegal products☆

Nahoko Uchiyama [a,*], Satoru Matsuda [a], Maiko Kawamura [a], Yoshihiko Shimokawa [a], Ruri Kikura-Hanajiri [a], Kosuke Aritake [b], Yoshihiro Urade [b], Yukihiro Goda [a]

[a] National Institute of Health Sciences, 1-18-1 Kamiyoga, Setagaya-ku, Tokyo 158-8501, Japan
[b] Department of Molecular Behavioral Biology, Osaka Bioscience Institute, 6-2-4 Furuedai, Suita-City, Osaka 565-0874, Japan

ARTICLE INFO

Article history:
Received 4 October 2013
Received in revised form 9 February 2014
Accepted 12 March 2014
Available online 27 March 2014

Keywords:
NNEI indazole analog
5-Chloro-NNEI
3,4-Dichloromethylphenidate
Synthetic cannabinoid
Cathinone derivative

ABSTRACT

Our continuous survey of illegal products in Japan revealed the new distribution of 15 designer drugs. We identified four synthetic cannabinoids, i.e., NNEI (**1**), 5-fluoro-NNEI (**2**), 5-chloro-NNEI (**3**) and NNEI indazole analog (**4**), and seven cathinone derivatives, i.e., MPHP (**5**), α-PHPP (**6**), α-POP (**7**), 3,4-dimethoxy-α-PVP (**8**), 4-fluoro-α-PVP (**9**), α-ethylaminopentiophenone (**10**) and *N*-ethyl-4-methyl-pentedrone (**11**). We also determined LY-2183240 (**12**) and its 2′-isomer (**13**), which were reported to inhibit endocannabinoid uptake, a methylphenidate analog, 3,4-dichloromethylphenidate (**14**), and an MDA analog, 5-APDB (**15**). No chemical and pharmaceutical data for compounds **3**, **4**, **6** and **7** had been reported, making this the first report on these compounds.

1. Introduction

A large number of new psychotropic substances continue to emerge around the world [1,2]. A total of 251 new psychotropic substances were identified by United Nations member states as of mid-2012. Most of the substances reported globally between 2009 and 2012 were synthetic cannabinoids (60 substances), followed by phenethylamines (58 substances) and synthetic cathinones (44 substances) [2]. We have been conducting an ongoing survey of designer drugs in the illegal drug market in Japan [3–8], and we reported the identification of newly distributed designer drugs among illegal products purchased in early 2013 that include the two synthetic cannabinoids 5-fluoro-QUPIC (5-fluoro-PB-22) and A-834735, a cathinone derivative, 4-methoxy-α-PVP, an opioid receptor agonist, MT-45 (I-C6), and a synthetic peptide, Noopept (GVS-111) [7]. Here we describe the identification of 15 newly distributed designer drugs (**1–15**, Fig. 1) among illegal products purchased in 2013.

2. Materials and methods

2.1. Samples for analyses

The analyzed samples were purchased on the Internet between January and August 2013 as chemical-type or herbal-type products A–L being sold in Japan. Each of the herbal-type products (A–C, J) contained about 3 g of mixed dried plants. Liquid-type products called "liquid aroma" were each about 5 ml of an orange liquid (D), a yellow liquid (F), a pale orange liquid (I) and a pale pink liquid (L). The powder-type products called "fragrance powder" were each about 400 mg of a brown powder (E), a white powder (G), a pale pink powder (H) or a white solid (K).

2.2. Chemicals and reagents

NNEI, 5-fluoro-NNEI, MPHP, 3,4-dimethoxy-α-PVP, α-ethylaminopentiophenone, α-PVP, LY-2183240, LY-2183240 2′-isomer, 5-APDB and 5-fluoro-QUPIC (5-fluoro-PB-22) were purchased from Cayman Chemicals (Ann Arbor, MI, USA). 8-Quinolinol was purchased from Tokyo Chemical Industry (Tokyo, Japan). Compounds **3**, **4**, and **9** were isolated from herbal or chemical products

☆ This paper is part of the special issue entitled "The 51st Annual Meeting of the International Association of Forensic Toxicologists (TIAFT)". September 2–3, 2013, Funchal, Medeira, Portugal. Guest edited by Professor Helena Teixeira, Professor Duarte Nuno Vieira and Professor Francisco Corte Real.

* Corresponding author at: National Institute of Health Sciences, Division of Pharmacognosy, Phytochemistry and Narcotics, 1-18-1 Kamiyoga, Setagaya-ku, Tokyo 158-8501, Japan. Tel.: +81 337 009 154; fax: +81 337 076 950.
E-mail address: nuchiyama@nihs.go.jp (N. Uchiyama).

http://dx.doi.org/10.1016/j.forsciint.2014.03.013
0379-0738/

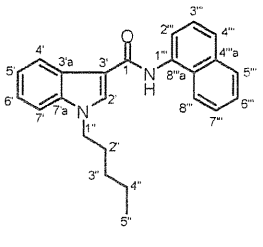

NNEI (MN-24, **1**)
$C_{24}H_{24}N_2O$: 356

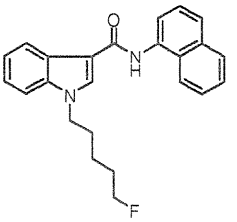

5-Fluoro-NNEI (5-Flouro-MN-24, **2**)
$C_{24}H_{23}FN_2O$: 374

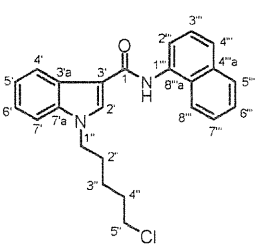

5-Chloro-NNEI (**3**)
$C_{24}H_{23}ClN_2O$: 391

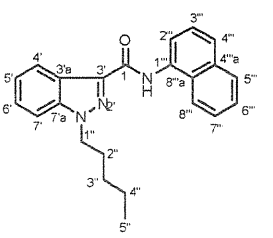

NNEI indazole analog (**4**)
[*N*-(Naphthalen-1-yl)-1-pentyl-1 *H*-indazole-3-carboxamide]
$C_{23}H_{23}N_3O$: 357

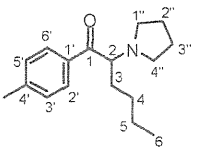

MPHP
(4-Methyl-α-pyrrolidinohexylphenone, **5**)
$C_{17}H_{25}NO$: 259

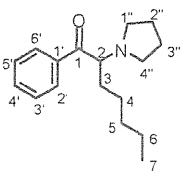

α-PHPP
(α-Pyrrolidinoheptanophenone, **6**)
$C_{17}H_{25}NO$: 259

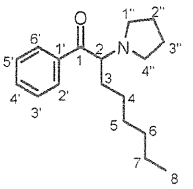

α-POP
(α-Pyrrolidino-octanophenone, **7**)
$C_{18}H_{27}NO$: 273

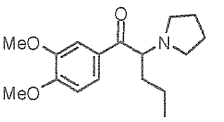

3,4-Dimethoxy-α-PVP (**8**)
$C_{17}H_{25}NO_3$: 291

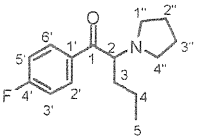

4-Fluoro-α-PVP (**9**)
$C_{15}H_{20}FNO$: 249

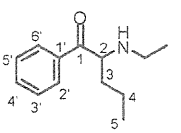

α-Ethylaminopentiophenone
(α-EAPP, **10**)
$C_{13}H_{19}NO$: 205

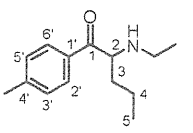

2-(Ethylamino)-1-(*p*-tolyl)pentan-1-one
(*N*-Ethyl-4-methyl-pentedrone,
4-Methyl-α-ethylaminopentiophenone, **11**)
$C_{14}H_{21}NO$: 219

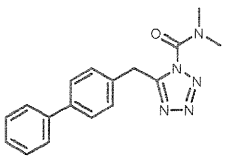

LY2183240 (**12**)
$C_{17}H_{17}N_5O$: 307

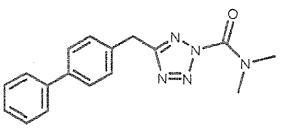

LY2183240 2'-isomer (**13**)
$C_{17}H_{17}N_5O$: 307

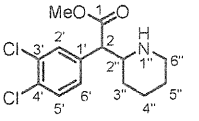

3,4-Dichloromethylphenidate (**14**)
$C_{14}H_{17}Cl_2NO_2$: 302

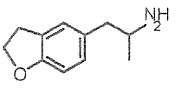

5-APDB (**15**)
$C_{11}H_{15}NO$: 177

Fig. 1. Structures of the new detected compounds (**1–15**).

as described below. All other common chemicals and solvents were of analytical reagent grade or HPLC grade. As solvents for the nuclear magnetic resonance (NMR) analysis, $CDCl_3$ (99.96%), pyridine-d_5 (99.96%) and dimethyl sulfoxide (DMSO)-d_6 (99.96%) were purchased from the ISOTEC division of Sigma–Aldrich (St. Louis, MO, USA).

2.3. Preparation of sample solutions

For the qualitative analyses, 10 mg of each herbal-type product was crushed into powder and extracted with 1 ml of methanol under ultrasonication for 10 min. A 2-mg portion of the powder-type product was extracted with 1 ml of methanol under ultrasonication for 10 min. A 20-μl portion of the liquid-type product was mixed with 1 ml of methanol under ultrasonication for 10 min. After the centrifugation (5 min, 3,000 rpm) of each extract, the supernatant solution was passed through a centrifugal filter (Ultrafree-MC, 0.45-μm filter unit; Millipore, Bedford, MA, USA) to serve as the sample solution for the analyses. If necessary, the solution was diluted with methanol to a suitable concentration before the instrumental analyses.

2.4. Analytical conditions

Each sample solution was analyzed by ultra-performance liquid chromatography–electrospray ionization–mass spectrometry

(UPLC–ESI–MS) and by gas chromatography–mass spectrometry (GC–MS) in the electron ionization (EI) mode according to our previous report [9]. Three elution programs were used in the LC–MS analysis. Program (1) was used for the synthetic cannabinoids, and program (2) was used for the other compounds including cathinone derivatives [9]. The elution program (3) was: 0.1% formic acid in water/0.1% formic acid in acetonitrile (80:20, v/v), 20-min hold. In this study, products A, B and C were analyzed using program (1), products E, F, G, H and I were analyzed using program (2), and product D was analyzed using program (3). Two programs were used in the GC–MS analysis, as follows. The oven temperature program (1), 80 °C (1-min hold) and an increase at a rate of 5 °C/min to 190 °C (15-min hold) followed by an increase at 10 °C/min up to 310 °C (20-min hold), and the oven temperature program (2), 150 °C (1-min hold) and increase at a rate of 20 °C/min to 280 °C (10-min hold) followed by an increase at 5 °C/min up to 310 °C (15-min hold). Program (2) was used for the analysis of product B. Other products were analyzed using program (1).

The obtained GC mass spectra were compared to those of an EI-MS library [Mass Spectra of Designer Drugs 2012 (Wiley-VCH, Weinheim, Germany)]. We also used our in-house EI-MS library of designer drugs obtained by our continuous survey of illegal products and commercially available reagents for the structural elucidation.

We measured the accurate mass numbers of the target compounds by liquid chromatography quadrupole-time-of-flight–mass spectrometry (LC–Q-TOF–MS) in the ESI mode according to our previous report [5].

For the isolation of each compound, we performed preparative gel permeation liquid chromatography (GPLC) on a JAI (Japan Analytical Industry, Tokyo, Japan) LC-9201 instrument with JAIGEL GS-310 columns or 1H columns (JAI) and 0.5% triethylamine (TEA) in methanol or chloroform as an eluent.

The NMR spectra were obtained on ECA-800 and 600 spectrometers (JEOL, Tokyo, Japan). Assignments were made via ^{1}H NMR, ^{13}C NMR, heteronuclear multiple quantum coherence (HMQC), heteronuclear multiple-bond correlation (HMBC), ^{15}N HMBC, double quantum filtered correlation spectroscopy (DQF-COSY), and rotating frame nuclear Overhauser effect (ROE) spectra.

2.5. Isolation of compound 3

A 3-g sample of mixed dried plants (product B) was extracted with 250 ml of chloroform by ultrasonication for 30 min. The extractions were repeated three times, and the supernatant fractions were combined and evaporated to dryness. The extract was loaded onto an ODS column (Bond Elute Mega Be-C18, 60 cm^3, 10 g; Agilent Technologies, Santa Clara, CA, USA), which was then eluted with a stepwise gradient of methanol–water (80:20–100:0). Then the extract was dissolved in 0.5% TEA in chloroform and purified by recycle GPLC (eluent: 0.5% TEA in chloroform) to give compound **3** (14 mg) as a white solid.

2.6. Isolation of compound 4

A 3-g sample of mixed dried plants (product J) was extracted with 250 ml of chloroform by ultrasonication for 30 min. The extractions were repeated three times, and the supernatant fractions were combined and evaporated to dryness. The extract was loaded onto a silica gel column (Bond Elute Mega SI, 60 cm^3, 10 g, Agilent Technologies), which was then eluted with a stepwise gradient of hexane-acetone. Then the extract was dissolved in 0.5% TEA in chloroform and purified by recycle GPLC (eluent: 0.5% TEA in chloroform) to give compound **4** (274 mg) as a yellow solid.

2.7. Isolation of compound 9

A 5-ml sample of liquid product L was evaporated to dryness, and then the extract was dissolved in 0.5% TEA in methanol and purified by recycle GPLC (eluent: 0.5% TEA in methanol) to give compound **9** (114 mg) as a yellow oil.

Compounds **6, 7, 11, 14** were directly analyzed without the isolation of products K, E, G and H.

3. Results and discussion

3.1. Identification of unknown peak 1

Unknown peak **1** was detected along with known 5-fluoro-QUPIC (5-fluoro-PB-22) and 8-quinolinol peaks in the LC–MS and GC–MS chromatograms for product A (Fig. 2a, b, e, g, j and k) [5,7]. Based on the GC–MS and LC–MS data, the unknown peak **1** was finally identified as a carboxamide derivative NNEI (Fig. 2c and h) by direct comparison of the data to those of the purchased authentic NNEI (Fig. 2d and i). NNEI (**1**), which was reported as a cannabinoid receptor agonist [10], was detected in illegal products in Russia and European countries in 2012 [1,11]. This is the first report of the detection of NNEI (**1**) as a newly distributed illegal drug in Japan.

3.2. Identification of unknown peaks 2 and 3

In the LC–MS analysis, unknown peaks **2** and **3** were detected in product B (Fig. 3a and b). However, in the GC–MS analysis using program (1), unknown peak **3** was not detected (Fig. 3f). Based on the GC–MS and LC–MS data, peak **2** was finally identified as 5-fluoro-NNEI (Fig. 3c and h) by direct comparison of the data to those of the purchased authentic compound (Fig. 3d and i). Compound **2** has also been detected in illegal products in Russia [11]. This is the first report of the detection of 5-fluoro-NNEI (**2**) as a newly distributed illegal drug in Japan.

Peak **3** at 27.6 min showed a putative molecular ion signal at *m/z* 390, and an isotopic ion signal at *m/z* 392 due to the presence of chlorine atom revealed by the GC–MS analysis using program (2) (Fig. 3g and j). The LC–MS data also suggested the presence of the chlorine atom in compound **3** due to the detected ion signals at *m/z* 391 $[M+H^+]$ and *m/z* 393 $[M+2+H^+]$ (Fig. 3e). After the isolation of unknown compound **3**, the accurate mass spectrum obtained by LC–Q-TOF–MS gave an ion peak at *m/z* 391.1573, suggesting that the protonated molecular formulae of compound **3** was $C_{24}H_{24}ClN_2O$ (calcd. 319.1577).

The ^{13}C NMR spectrum of compound **3** was very similar to that of NNEI (**1**) except for the Cl-substituted moiety (C-5″) of compound **3**, as shown in Table 1. On the basis of the mass spectra and the observed DQF-COSY, HMBC and 1D-ROE correlations shown in Figs. 3e and j and 4a, we identified the structure of compound **3** as 5-chloro-NNEI (IUPAC: 1-(5-chloropentyl)-*N*-(naphthalen-1-yl)-1*H*-indole-3-carboxamide) (Fig. 1). Compound **3** is a novel cannabimimetic substance and its chemical and pharmaceutical data have not been reported, although its structure is similar to that of NNEI (**1**) [10].

3.3. Identification of unknown peaks 4, 6, 12 and 13

Four unknown peaks, **4**, **6**, **12** and **13**, were detected in the LC–MS and GC–MS chromatograms for product C (Fig. 5a, b and i). In the LC–MS analysis, the unknown peak **4** at 13.1 min showed a protonated molecular ion signal at *m/z* 358 ($[M+H]^+$) (Fig. 5c). The other unknown peak **6** at 2.2 min showed a major ion peak at *m/z* 260 ($[M+H]^+$) (Fig. 5d). The UV spectra of compounds **4** and **6** showed absorbance maxima at 309 and 253 nm (Fig. 5c and d).

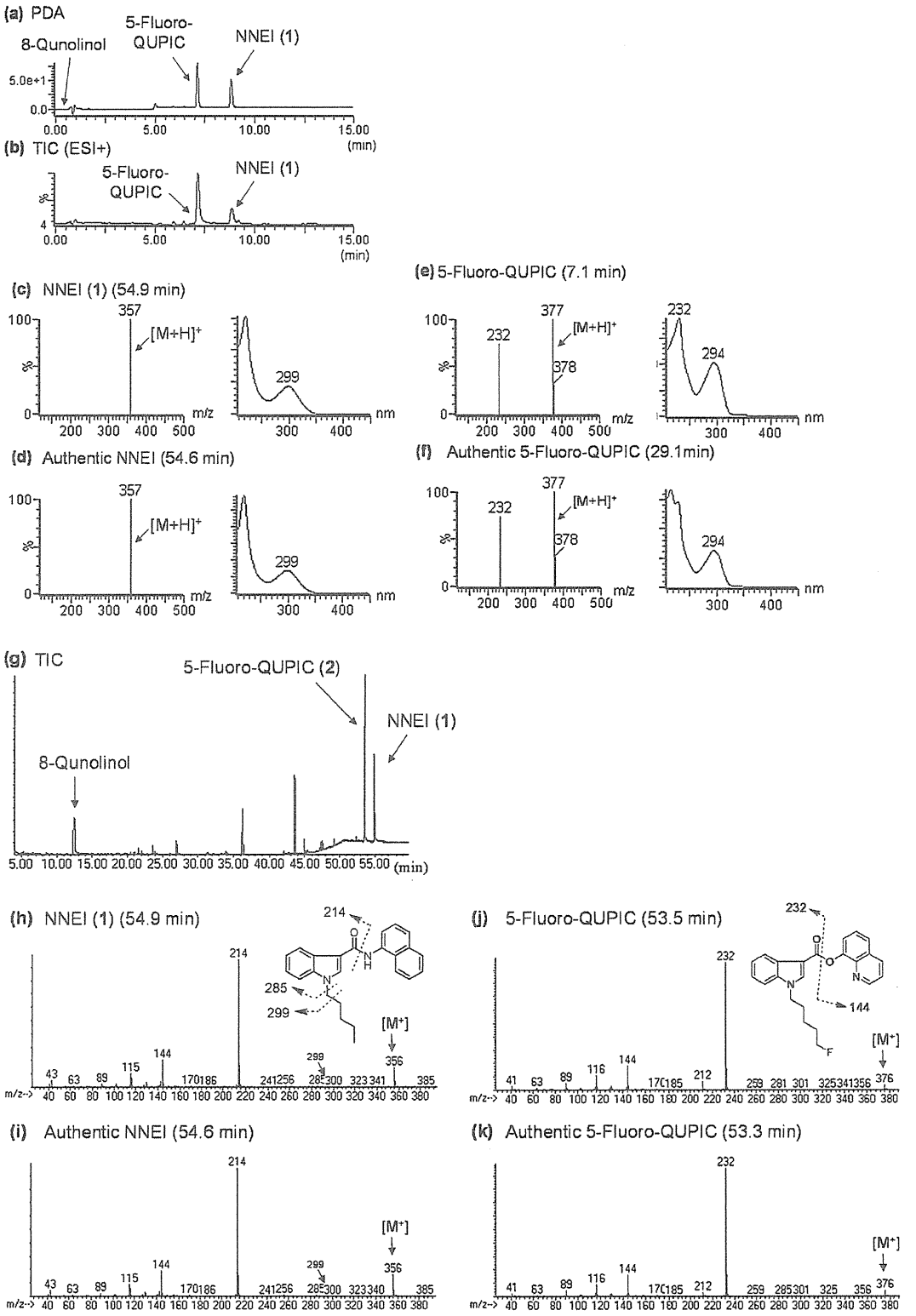

Fig. 2. LC–MS and GC–MS analyses of product A. LC–UV–PDA chromatogram (a) and total ion chromatogram (TIC) (b). ESI mass and UV spectra of peaks **1** (c), 5-fluoro-QUPIC (e), authentic NNEI and 5-fluoro-QUPIC (d and f, respectively). TIC (g) and EI mass spectra of peaks **1** (h), 5-fluoro-QUPIC (j) and authentic NNEI and 5-fluoro-QUPIC (i and k, respectively) obtained by GC–MS analysis.

The LC–MS and GC–MS analyses revealed that products J and K contained mostly compounds **4** and **6**, respectively. Therefore, product K was directly analyzed as compound **6**, though compound **4** was further purified from product J. The accurate mass spectra of compounds **4** and **6** were measured by LC–TOF–MS in the positive mode. The ion peaks observed at *m/z* 358.1905 and 260.2020 suggested that the protonated molecular formula of compounds **4** and **6** were $C_{23}H_{24}N_3O$ (calcd. 358.1919) and $C_{17}H_{26}NO$ (calcd. 260.2014), respectively.

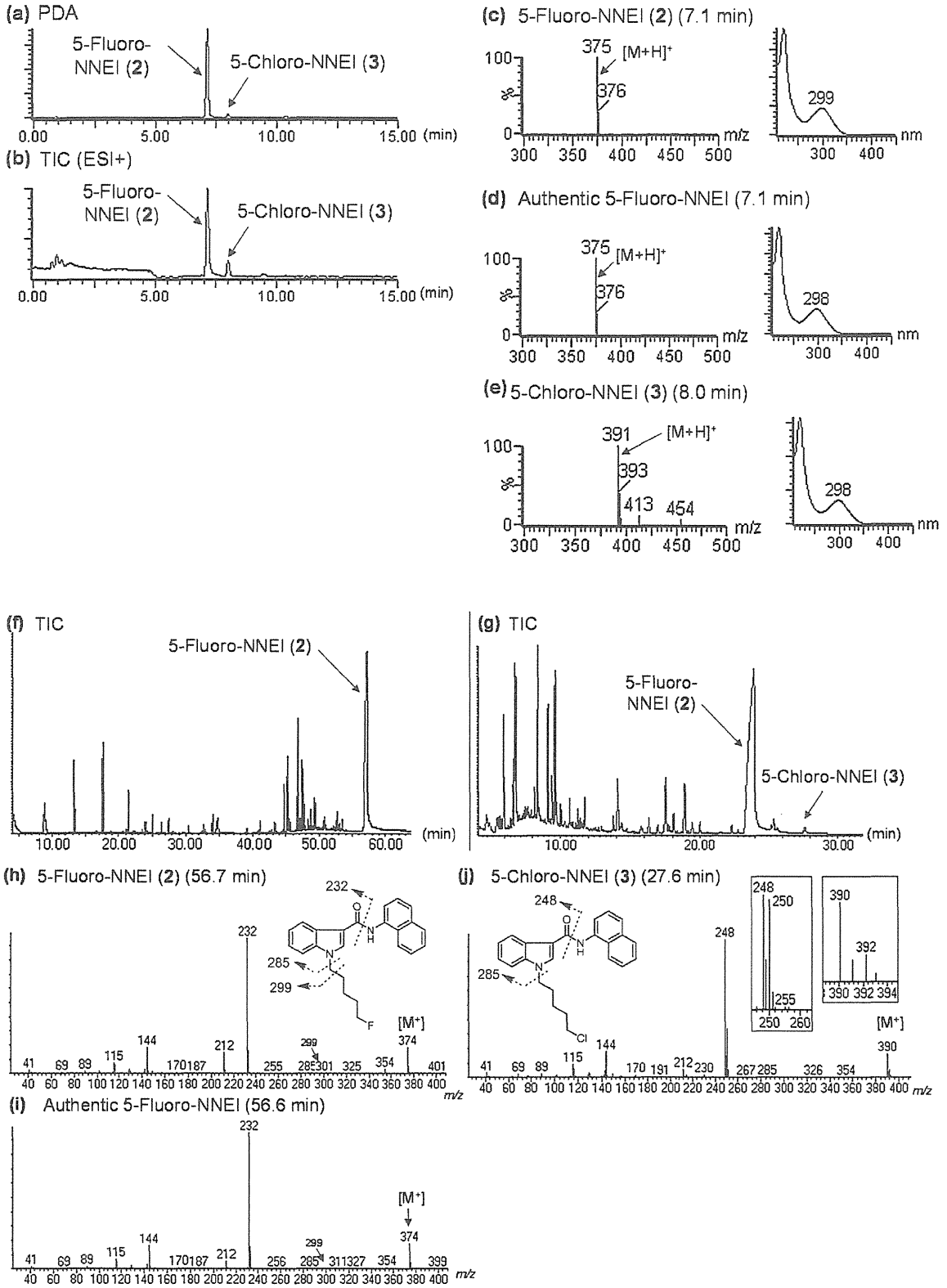

Fig. 3. LC–MS and GC–MS analyses of product B. LC–UV–PDA chromatogram (a) and TIC (b). ESI mass and UV spectra of peaks **2** (c), **3** (e) and authentic 5-fluoro-NNEI (d). TIC (f, g) and EI mass spectra of peaks **2** (h), **3** (j) and authentic 5-fluoro-NNEI (i) obtained by the GC–MS analysis.

The structure of compound **4** was elucidated by NMR analysis (Table 1, Fig. 4b and c). The ^{13}C NMR spectra of compound **4** was similar to that of NNEI (**1**), except for an indole moiety (position-2′ to 7′a) of NNEI (**1**) as shown in Table 1. The difference between the molecular formula of compound **4** ($C_{23}H_{23}N_3O$) and that of NNEI (**1**) ($C_{24}H_{24}N_2O$) is the additional nitrogen atom in the place of the absent C_1H_1. The comparison of ^1H and ^{13}C NMR data between compounds **4** and **1** revealed the loss of the methine unit at the

Table 1
NMR data of NNEI (**1**), 5-chloro-NNEI (**3**) and NNEI indazole analog (**4**).

No.	NNEI (**1**)[a]	5-Chloro-NNEI (**3**)[b]		NNEI indazole analog (**4**)[b]	
	^{13}C	^{13}C	^{1}H	^{13}C	^{1}H
1	164.0	163.9	–	160.9	–
2′	132.3	132.1	7.83, 1H, brs	–	–
3′	110.9	111.1	–	137.3	–
3′a	125.5	125.6	–	123.0	–
4′	122.7	122.8	7.34, 1H, m, overlapped	122.9	8.92, 1H, d, J = 8.3 Hz
5′	121.9	122.0	7.32, 1H, m, overlapped	122.9	7.78, 1H, ddd, J = 7.3, 6.9 Hz
6′	120.1	120.3	8.13, 1H, m, overlapped	126.9	7.91, 1H, td, J = 7.3, 0.9 Hz
7′	110.6	110.5	7.43, 1H, m	109.4	7.93, 1H, brd, J = 8.3 Hz
7′a	136.7	136.7	–	141.1	–
1″	47.0	46.8	4.20, 2H, t, J = 7.2 Hz	49.6	4.93, 2H, t, J = 7.3 Hz
2″	29.6	29.3	1.92, 2H, q, J = 7.2 Hz	29.5	2.48, 2H, q, J = 7.3 Hz
3″	29.0	24.2	1.50, 2H, m	29.0	1.86, 2H, m, overlapped
4″	22.3	32.0	1.80, 2H, q, J = 6.9 Hz	22.3	1.83, 2H, m, overlapped
5″	13.9	44.6	3.51, 2H, t, J = 6.9 Hz	14.0	1.37, 3H, t, J = 7.3 Hz
1‴	132.9	132.9	–	132.4	–
2‴	121.0	121.0	8.08, 1H, d, J = 7.2 Hz	119.4	8.79, 1H, d, J = 7.3 Hz
3‴	125.9	125.9	7.52, 1H, m, overlapped	126.0	8.00, 1H, t, J = 7.8 Hz
4‴	125.6	125.6	7.72, 1H, d, J = 8.3 Hz	125.0	8.16, 1H, d, J = 8.3 Hz
4‴a	134.2	134.2	–	134.2	–
5‴	128.8	128.8	7.89, 1H, dd, J = 7.6, 1.7 Hz	128.8	8.35, 1H, d, J = 7.8 Hz
6‴	126.0	126.0	7.50, 1H, td, J = 6.9, 1.4 Hz, overlapped	125.9	7.98, 1H, ddd, J = 7.8, 7.3. 0.9 Hz
7‴	126.3	126.4	7.53, 1H, td, J = 6.9, 1.4 Hz, overlapped	126.2	8.03, 1H, ddd, J = 8.9, 8.3, 1.4 Hz
8‴	120.8	120.9	7.98, 1H, d, J = 8.3 Hz	120.5	8.52, 1H, d, J = 8.3 Hz
8‴a	127.4	127.4	–	126.7	–
NH	–	–	8.12, 1H, brs, overlapped	–	9.90, 1H, s

[a] Recorded in $CDCl_3$ at 800 MHz (^{1}H) and 200 MHz (^{13}C), respectively; data in δ ppm (J in Hz).
[b] Recorded in $CDCl_3$ at 600 MHz (^{1}H) and 150 MHz (^{13}C), respectively; data in δ ppm (J in Hz).

2′-positon of the indole group of compound **1** in the structure of compound **4**. In addition, the major fragment ions at m/z 215 and 300 of peak **4** instead of those at m/z 214 and 299 of peak **1** (Figs. 2i and 5j) shown by the GC–MS analyses strongly suggested the replacement of the methine unit with a nitrogen atom. On the basis of the mass spectra and the observed DQF-COSY, HMBC, ^{15}N HMBC and 1D-ROE correlations shown in Figs. 4b and c and 5j, we identified the structure of compound **4** as an NNEI indazole analog [IUPAC: *N*-(naphthalen-1-yl)-1-pentyl-1*H*-indazole-3-carboxamide] (Fig. 1).

The proposed fragment patterns and presumed structure of compound **6** as revealed by the GC–MS analysis are also shown in Fig. 5k. The ^{13}C NMR spectrum of compound **6** was very similar to that of a cathinone derivative, α-PVP, except for the additional C_2H_5 of an *n*-alkyl moiety (position-6 to 7) of compound **6** as shown in Table 2. The observed ^{1}H and ^{13}C NMR (Tables 2 and 3), DQF-COSY, HMBC and 1D-ROE correlations (data not shown) revealed that the structure of compound **6** is α-Pyrrolidinoheptanophenone (α-PHPP) as shown in Fig. 1. In addition, the fragment ions at m/z 77, 105 and 154 of compound **6** in the GC–MS spectrum as shown in Fig. 5k further confirmed the structure. Compounds **4** and **6** were detected as novel substances and their chemical and pharmaceutical data have not been reported.

The remaining unknown peaks **12** and **13** were identified as LY-2183240 (Fig. 5e and l) and LY-2183240 2′-isomer (Fig. 5g and n), respectively by a direct comparison of the data with those of the purchased authentic compounds (Fig. 5f and m; Fig. 5h and o, respectively). LY-2183240 (**12**) was reported to have a potent, competitive inhibitory effect of endocannabinoid (anandamide) uptake (IC_{50} = 270 pM; K_i = 540 pM) and hydrolysis, and to increase endocannabinoid (anandamide) levels in rat cerebellum

Table 2
^{13}C NMR Data of compounds **6**, **7**, **9** – **11** and α-PVP.

No.	α-PVP[a]	α-PHPP (**6**)[a]	α-POP (**7**)[a]	4-Fluoro-α-PVP (**9**)[a]	α-EAPP (**10**)[b]	*N*-Ethyl-4-methyl-pentedrone (**11**)[c]
1	198.9	198.7	198.7	198.9	196.4	195.8
2	66.8	66.8	66.8	69.3	60.5	60.3
3	32.1	30.1	30.1	31.5	31.8	31.9
4	19.7	25.9	26.2	19.9	17.2	17.2
5	14.2	31.9	29.5	14.3	13.6	13.7
6	–	22.5	31.6	–	–	–
7	–	14.0	22.7	–	–	–
8	–	–	14.1	–	–	–
1′	137.0	136.9	137.0	133.8, d, J = 2.9 Hz[d]	133.9	131.5
2′/6′	129.2	129.2	129.2	132.1, d, J = 8.7 Hz[d]	128.7	128.9
3′/5′	129.3	129.3	129.3	115.8, d, J = 21.7 Hz[d]	129.2	129.8
4′	134.1	134.2	134.2	165.8, d, J = 252.9 Hz[d]	134.8	145.7
2″/5″	51.2	51.3	51.3	50.6	–	–
3″/4″	24.0	24.0	24.0	23.8	–	–
N-$\underline{C}H_2CH_3$	–	–	–	–	41.2	41.2
N-$CH_2\underline{C}H_3$	–	–	–	–	11.2	11.2
4′-Me	–	–	–	–	–	21.3

[a] Recorded at 600 MHz (^{1}H) and 150 MHz (^{13}C), respectively; data in δ ppm (J in Hz).
[b] Recorded in pyridine-d_5.
[c] Recorded in DMSO-d_6.
[d] Observed as double signals by coupling with fluorine.

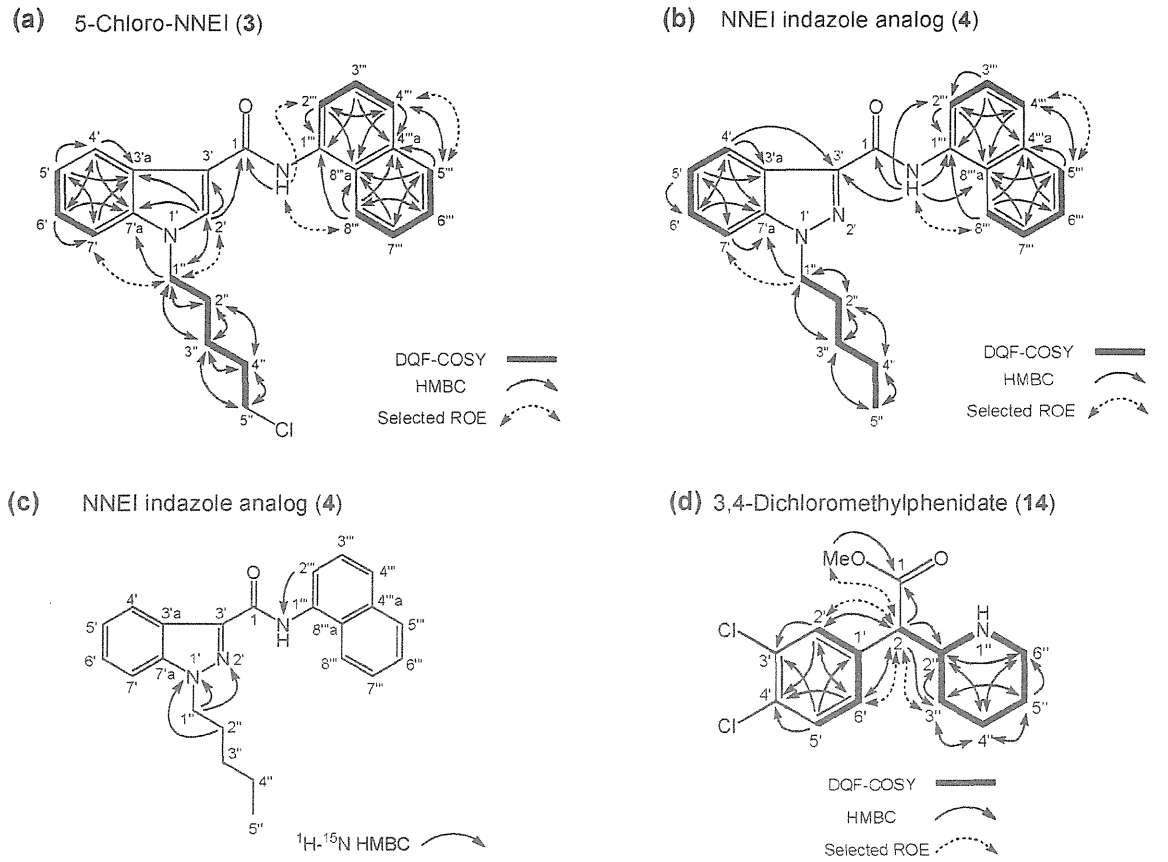

Fig. 4. DQF-COSY, selected HMBC, and selected ROE correlations (a) for compound **3** (5-chloro-NNEI), and DQF-COSY, selected HMBC and selected ROE correlations for compound **4** (NNEI indazole analog, b) and compound **14** (3,4-Dichloromethylphenidate, d). ^{1}H–^{15}N HMBC correlation for compound **4** (NNEI indazole analog, c).

[12]. LY-2183240 2′-isomer was reported to have a less potent inhibitory effect of endocannabinoid uptake (IC_{50} = 998 nM) and hydrolysis [13]. Compounds **12** and **13** were detected as newly distributed designer drugs.

3.4. Identification of unknown peaks 5 and 8

We detected two unknown peaks, **5** and **8**, with α-PHPP (**6**) in the LC–MS using elution program (3) and GC–MS chromatograms for product D (Fig. 6a, b and g). Peaks **5** and **8** were identified as the cathinone derivatives MPHP (Fig. 6c and h) and 3,4-dimethoxyl-α-PVP (Fig. 6e and j), respectively, by direct comparison of the data with those of the purchased authentic compounds (Fig. 6d, i, f and k).

The appearance of MPHP (**5**) on the German illegal drug market was reported [14]. Saurer et al. reported that MPHP intake can lead to serious poisoning with toxic liver damage and rhabdomyolysis [15]. Compound **8** was reported as a

Table 3
^{1}H NMR data of compounds **6**, **7**, **9** and **11**.

No.	α-PHPP (**6**)[b]	α-POP (**7**)[b]	4-Fluoro-α-PVP (**9**)[b]	*N*-Ethyl-4-methylpentedrone (**11**)
1	–	–	–	–
2	5.02, 1H, brs	5.03, 1H, brs	4.88, 1H, brs	5.20, 1H, brs
3	2.09, 2H, m	2.11, 2H, m	2.05, 2H, m	1.85, 2H, m
4	1.35, 2H, m	1.37, 2H, m	1.36, 2H, m	1.27, 1H, m, overlapped 1.05, 1H, m
5	1.09, 2H, m, overlapped	1.12, 2H, m, overlapped	0.77, 3H, t, J = 7.4 Hz	0.76, 3H, t, J = 7.2 Hz
6	1.07, 2H, m, overlapped	1.02, 2H, m, overlapped	–	–
7	0.69, 3H, t, J = 7.2 Hz	1.08, 2H, m, overlapped	–	–
8	–	0.72, 3H, t, J = 7.6 Hz	–	–
1′	–	–	–	–
2′/6′	8.32, 2H, t, J = 7.6 Hz	8.33, 2H, dd, J = 8.6, 1.4 Hz	8.35, 2H, d, J = 8.7 Hz	7.97, 2H, d, J = 7.9 Hz
3′/5′	7.49, 2H, t, J = 7.6 Hz	7.50, 2H, t, J = 8.6 Hz	7.06, 2H, d, J = 8.7 Hz	7.41, 2H, d, J = 7.9 Hz
4′	7.57, 1H, t, J = 7.6 Hz	7.58, 1H, tt, J = 8.6, 1.4 Hz	–	–
2″/5″	3.27, 3.08, each 2H, brs	3.28, 3.10, each 2H, brs	3.23, 3.03, each 2H, brs	–
3″/4″	1.79, 4H, m	1.80, 4H, m	1.77, 4H, m	–
N-CH_2CH_3	–	–	–	2.99, 2.89, each 1H, m
N-CH_2CH_3	–	–	–	1.22, 3H, t, J = 7.2 Hz
4′-Me	–	–	–	2.40, 3H, s

[a] Recorded at 600 MHz (^{1}H) and 150 MHz (^{13}C), respectively; data in δ ppm (J in Hz)
[b] Recorded in pyridine-d_5.
[c] Recorded in DMSO-d_6.

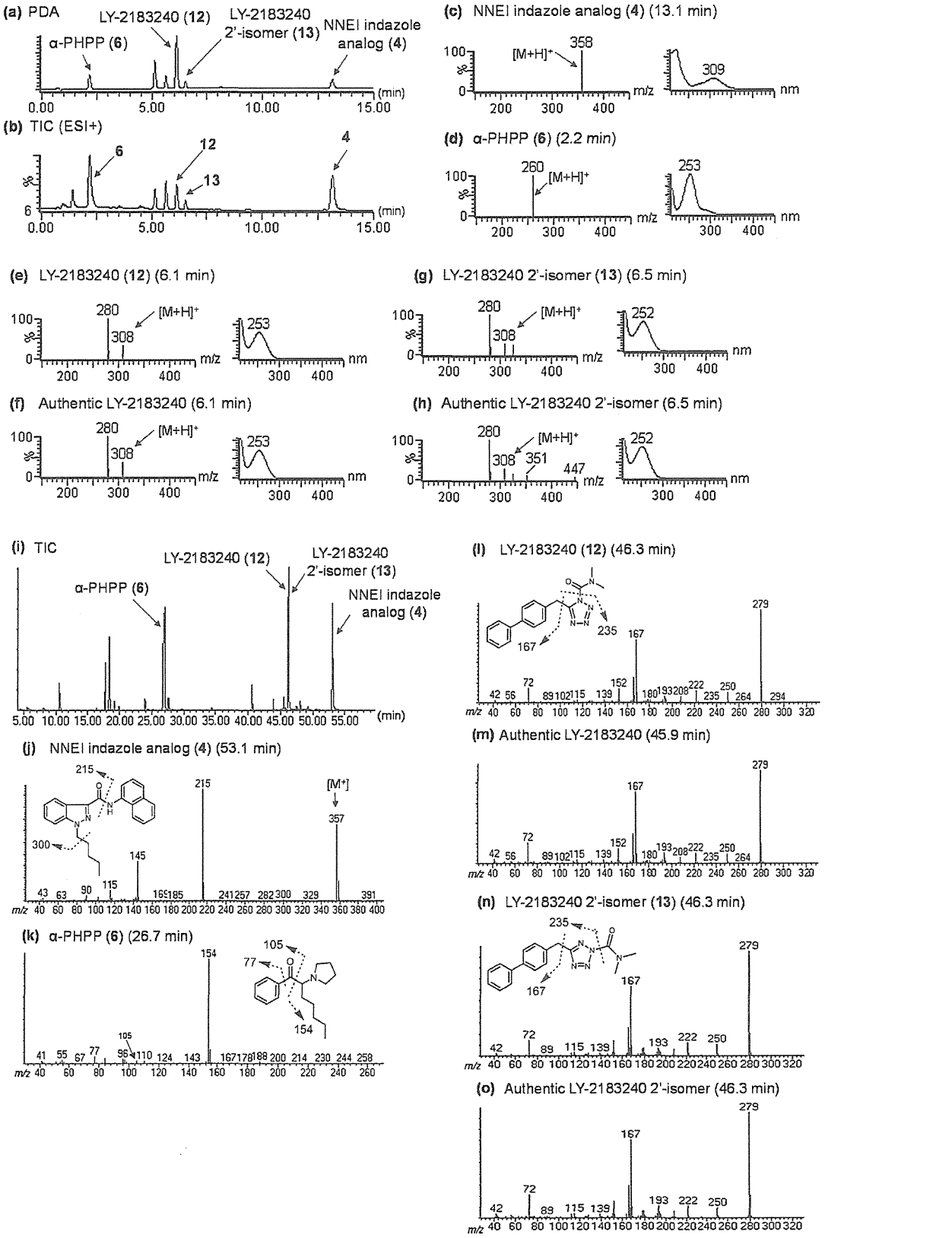

Fig. 5. LC–MS and GC–MS analyses of product C. LC–UV–PDA chromatogram (a) and TIC (b). ESI mass and UV spectra of peaks **4** (c), **6** (d), **12** (e), **13** (g) and authentic LY-2183240 and LY-2183240 2′-isomer (f and h), respectively. TIC (**i**) and EI mass spectra of peaks **4** (i), **6** (k), **12** (l), **13** (m) and authentic LY-2183240 and LY-2183240 2′-isomer (n and o), respectively, obtained by the GC–MS analysis.